Synthesis and Reactivity of Early−Late Heterodinuclear Complexes Stabilized by a Trisilylsilane-Based Tripodal Amido Ligand[†]

Lutz H. Gade,*,‡ Martin Schubart,§ Bernd Findeis,§ Sylvie Fabre,§ Izoldi Bezougli,§ Matthias Lutz,§ Ian J. Scowen,‖ and Mary McPartlin‖

Laboratoire de Chimie Organométallique et de Catalyse, Institut LeBel, Université Louis Pasteur, 4 rue Blaise Pascal, 67070 Strasbourg, France, Institut für Anorganische Chemie der Universität Würzburg, Am Hubland, 97074 Würzburg, Germany, and School of Applied Chemistry, University of North London, Holloway Road, London N7 8DB, U.K.

Received March 10, 1999

The reaction of the complexes [MeSi{SiMe$_2$N(R)}$_3$MX] (R = *p*-tolyl, 2-FC$_6$H$_4$; M = Ti, Zr, Hf; X = Cl, Br) with K[CpM′(CO)$_2$] afforded the metal−metal bonded heterodinuclear complexes [MeSi{SiMe$_2$N(R)}$_3$M−M′(CO)$_2$Cp] (M = Ti, Zr, Hf; M′ = Fe, Ru; R = *p*-tolyl, 2-C$_6$H$_4$), all of which are thermally stable in the solid state and in solution. X-ray crystal structure analyses of the complexes [MeSi{SiMe$_2$N(*p*-tol)}$_3$M−M′(CO)$_2$Cp] (M, M′: Ti, Fe (**3**); Ti, Ru (**4**); Zr, Fe (**5**)) and [MeSi{SiMe$_2$N(2-FC$_6$H$_4$)}$_3$Ti−Fe(CO)$_2$Cp] (**9**) established the presence of unsupported metal−metal bonds [**3**, Ti−Fe 2.460(1); **4**, Ti−Ru 2.5609(8); **5**, Zr−Fe 2.605(2); **9**, Ti−Fe 2.433(4) Å]. Reaction of the dinuclear complexes with isonitriles led to insertion of the substrate into the polar metal−metal bond and the formation of the metallaiminoacyl complexes [MeSi{SiMe$_2$N(R)}$_3$M{η^2-(C=NR′)M′(CO)$_2$Cp}] (M = Ti, Zr, Hf; M′ = Fe, Ru; R = *p*-tolyl, 2-C$_6$H$_4$; R′ = Me, *p*-tolyl). The ^{13}C NMR resonances of the isonitrile-derived carbon nuclei linking the two metal centers are observed at remarkably low field (δ 267.8−303.8). The structural proposal for the insertion products was confirmed by an X-ray crystallographic study of [MeSi{SiMe$_2$N(*p*-tol)}$_3$Ti{η^2-(C=NMe)Ru(CO)$_2$Cp}]. When the heterobimetallic complex [MeSi{SiMe$_2$N(*p*-tol)}$_3$Zr−Ru(CO)$_2$Cp] was reacted with sulfoxides [Me$_2$SO, Me(Ph)SO, (PhCH$_2$)$_2$SO, (CH$_2$)$_4$SO], immediate oxygen transfer to a carbonyl ligand occurred, generating the dinuclear complexes [MeSi(SiMe$_2$NTol)$_3$Zr(μ-O$_2$C)RuCp(CO){S(R)R′}] (R = R′ = Me (**23a**); R = Me, R′ = Ph (**23b**); R, R′ = (CH$_2$)$_4$ (**23c**); R, R′ = PhCH$_2$ (**23d**)), in which the two metal centers are linked by a CO$_2$ ligand derived from a carbonyl ligand in the starting material. In the presence of a second equivalent of sulfoxide, the Lewis acid−base adducts [MeSi(SiMe$_2$NTol)$_3$Zr{OS(R)R′-κO}(μ-O$_2$C)RuCp(CO){S(R)R′}] (R = R′ = Me (**24a**); R = Me, R′ = Ph (**24b**); R, R′ = (CH$_2$)$_4$ (**24c**)) were formed. An X-ray crystal structure analysis of **24a** established the conversion of the carbonyl ligand to the bridging matallacarboxylate unit and the coordination of the thioether, formed in the oxygen transfer, to the Ru atom. The oxygen transfer from the sulfoxide to a carbonyl ligand was confirmed by an NMR study of the reaction using ^{13}C-labeled carbonyl derivatives and ^{17}O-labeled Me(Ph)SO.

Introduction

The principal concepts related to the bimetallic activation of molecules by complementary metal centers were formulated in the 1970s.[1,2] In particular, the synthesis of complexes containing direct metal−metal bonds between the elements of the two extreme ends of the d block in the periodic system was attempted by several research groups.[3−7] The underlying aim was to cleave these metal−metal bonds under controlled conditions and thus make available a pair of complementary reactive complex fragments which were expected to react in a cooperative way with organic substrates.[8−13]

Moreover, it was of fundamental interest to investigate the characteristics of the bonding situation between metal centers possessing significantly different electronic properties. Particularly important to the development of this field, among the early contributions to the regime of directly metal−metal bonded "early−late heterobimetallics", were the Zr−Ru and Zr−Fe complexes reported by Casey (**A**) and co-workers[14−18] as well as the Ti−Fe and Ti−Ru complexes studied in Selegue's group

---

[†] Dedicated to Professor John A. Osborn, a colleague and friend, on the occasion of his 60th birthday.

‡ Université Louis Pasteur. E-mail: gade@chimie.u-strasbg.fr.

§ Universität Würzburg.

‖ University of North London.

(1) Roberts, D. A.; Geoffroy, G. L. In *Comprehensive Organometallic Chemistry*; Wilkinson, G., Stone, F. A. G., Abel, E. W., Eds.; Pergamon: Oxford, 1982; Vol. 6, p 763.

(2) Braunstein, P.; Rose, J. In *Stereochemistry of Organometallic and Inorganic Compounds*; Bernal, I., Ed.; Elsevier: Amsterdam, 1989; Vol. 3, p 3.

(3) Cardin, D. J.; Keppie, S. A.; Lappert, M. F. *J. Chem. Soc. A* **1970,** 2594.

(4) Lappert, M. F.; Sanger, A. R. *J. Chem. Soc. A* **1971,** 1314.

(5) Schmid, G.; Stutte, B.; Boese, R. *Chem. Ber.* **1978,** *111,* 1239.

(6) Marsella, J. A.; Huffman, J. C.; Caulton, K. G.; Norton, J. R. *J. Am. Chem. Soc.* **1982,** *104,* 6360.

(7) Stephan, D. W. *Coord. Chem. Rev.* **1989,** *95,* 41.

(8) Ferguson, G. S.; Wolczanski, P. T.; Parkanyi, L.; Zonnevylle, M. *Organometallics* **1988,** *7,* 1967.

(9) Ozawa, F.; Park, J. W.; Mackenzie, P. B.; Schaefer, W. P.; Henling, L. M.; Grubbs, R. H. *J. Am. Chem. Soc.* **1989,** *111,* 1319.

(10) Baranger, A. M.; Bergman, R. G. *J. Am. Chem. Soc.* **1994,** *116,* 3822.

(11) Hanna, T. A.; Baranger, A. M.; Bergman, R. G. *J. Am. Chem. Soc.* **1995,** *117,* 665.

(12) Baranger, A. M.; Hanna, T. A.; Bergman, R. G. *J. Am. Chem. Soc.* **1995,** *177,* 10041.

(13) Hanna, T. A.; Baranger, A. M.; Bergman, R. G. *J. Am. Chem. Soc.* **1995,** *117,* 11363.

Chart 1

(**A**)   (**B**)   (**C**)
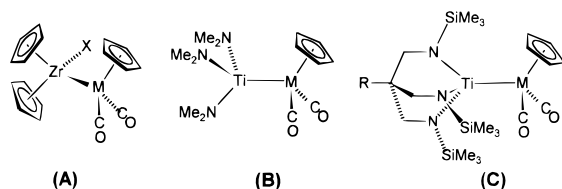
(**B**).[19−22] (See Chart 1.) However, a systematic investigation of the structural and reactive consequences of high metal−metal bond polarity was hampered for a long time by the instability of the systems which were available.

On the basis of Selegue's concept of employing amidotitanium complex units for the synthesis of unsupported early−late heterodinuclear complexes, we attempted to overcome the stability problem by the development of several new types of tripodal amido ligands[23−26] to be used in the early transition metal "building blocks" (**C**).[27,28] Not only were these designed to meet the electronic demands of a high-valent Lewis acidic metal center by nature of the σ- and π-donor capability, but also the ligand backbone and the peripheral groups bound to the amido N atoms were intended to sterically shield a large part of the coordination sphere and thus kinetically stabilize the dinuclear complexes.[29,30] In addition, the integration of the early transition metal center into the rigid [2.2.2]bicyclooctane-related cage structure provides a significant additional thermodynamic component to the stability of the heterodinuclear complexes since the geometrical relaxation of the early transition metal fragment to a trigonal planar arrangement upon dissociation of the metal−metal bond is impeded by the polydentate ligand. In other words, one of the fragments generated after the rupture of the metal−metal bond is destabilized in comparison to those derived from complexes coordinated by monodentate amides. A detailed theoretical study performed on Ti−Co compounds provided an estimate of ca. 10 kcal mol^{-1} for this stabilization of the molecules.[31]

The practical implementation of these considerations was achieved recently, and a trisilylsilane-derived amido ligand system was found to be particularly suited for the stabilization of a whole series of Ti−M, Zr−M, and Hf−M complexes (M = Fe, Ru, Co). In this paper, we provide a detailed account of

the synthesis and the structural characterization as well as some aspects of the reactive behavior of such metal−metal bonded heterodinuclear compounds.[32,33]

Experimental Section

All manipulations were performed under an inert gas atmosphere of dried argon in standard (Schlenk) glassware which was flame-dried with a Bunsen burner prior to use. Solvents were dried according to standard procedures and saturated with Ar. The deuterated solvents used for the NMR spectroscopic measurements were degassed by three successive "freeze−pump−thaw" cycles and dried over 4 Å molecular sieves.

The ^{1}H, ^{13}C, ^{29}Si, ^{19}F, and ^{31}P NMR spectra were recorded on a Bruker AC 200 spectrometer equipped with a B-VT-2000 variable-temperature unit (at 200.13, 50.32, 39.76, 188.31, and 81.03 MHz, respectively) with tetramethylsilane and H$_3$PO$_4$ (85%, external) as references. All spectra were recorded at 295 K unless specified otherwise. Infrared spectra were recorded on Perkin-Elmer 1420 and Bruker IRS 25 FT spectrometers.

Elemental analyses were carried out in the microanalytical laboratory of the chemistry department of the University of Würzburg. The complexes [MeSi{SiMe$_2$N(*p*-tol)}$_3$MX] (M/X: Ti/Br, **1a**; Zr/Cl, **1b**; Hf/Cl, **1c**) and [MeSi{SiMe$_2$N(2-C$_6$H$_4$)}$_3$MX] (M/X: Ti/Br, **2a**; Zr/Cl, **2b**; Hf/Cl, **2c**) were prepared as reported previously by us.[26,28] The salts of the transition metal carbonylates K[CpFe(CO)$_2$] and K[CpRu(CO)$_2$] were synthesized by literature methods.[34] All other chemicals used as starting materials were obtained commercially and used without further purification.

(1) General Procedure for the Synthesis of the Heterodinuclear Complexes [MeSi{SiMe$_2$N(*p*-tol)}$_3$Ti−M′(CO)$_2$Cp] (M′ = Fe, Ru). To a mixture of solid [MeSi{SiMe$_2$N(*p*-tol)}$_3$TiBr] (**1a**, 570 mg = 0.86 mmol) and 0.86 mmol of solid K[M′Cp(CO)$_2$] was slowly added 20 mL of toluene, which was precooled at −60 °C. The reaction mixture was stirred, warmed to ambient temperature over a period of 10 h, and stirred at 30 °C for another 24 h. The solvent was subsequently removed in vacuo, the residue was extracted with 20 mL of pentane, and the extract was filtered. The filtrate was concentrated to ca. 5 mL and stored at −30 °C. Compounds **3** and **4** were obtained as yellow crystalline solids.

(a) [MeSi{SiMe$_2$N(*p*-tol)}$_3$Ti−Fe(CO)$_2$Cp] (3). Yield: 320 mg (49%). Mp: 62 °C. ^{1}H NMR (C$_6$D$_6$) δ: 0.02 (s, 3H, CH$_3$Si), 0.46 (s, 18H, Si(CH$_3$)$_2$), 2.21 (s, 9H, C*H*$_3$C$_6$H$_4$), 3.46 (s, 5H, C$_5$H$_5$), 7.15 (m, 12H, Tol). ^{13}C{^{1}H} NMR (C$_6$D$_6$): δ = −13.8 (CH$_3$Si), 2.7 (Si(CH$_3$)$_2$), 20.9 (CH$_3$C$_6$H$_4$), 85.3 (C$_5$H$_5$), 117.0 (C^2), 129.5 (C^3), 132.3 (C^4), 150.8 (C^1), 214.2 (CO). IR (toluene): ν(CO) 1978, 1931 cm^{-1}. Anal. Calcd for C$_{35}$H$_{47}$FeN$_3$O$_2$Si$_4$Ti: C, 55.47; H, 6.25; N, 5.54. Found: C, 55.15; H, 6.22; N, 5.25.

(b) [MeSi{SiMe$_2$N(*p*-tol)}$_3$Ti−Ru(CO)$_2$Cp] (4). Yield: 180 mg (26%). Mp: 114 °C dec. ^{1}H NMR (C$_6$D$_6$, 320 K): δ = 0.06 (s, 3H, C*H*$_3$Si), 0.44 (s, 18H, Si(C*H*$_3$)$_2$), 2.19 (s, 9H, C*H*$_3$C$_6$H$_4$), 4.02 (s, 5H, C$_5$H$_5$), 7.23 (d, $^3J_{HH}$ = 7.8 Hz, 6H, H^{2,6}) 7.50 (d, 6H, H^{3,5}). ^{13}C{^{1}H} NMR (C$_6$D$_6$, 295 K): δ = −13.7 (CH$_3$Si), 2.6 (Si(CH$_3$)$_2$), 20.8 (CH$_3$C$_6$H$_4$), 87.4 (Cp), 126.7 (C^2), 129.9 (C^3), 132.3 (C^4), 149.4 (C^1), 203.4 (CO). IR (Nujol): ν(CO) 1991, 1937 cm^{-1}. Anal. Calcd for C$_{35}$H$_{47}$N$_3$O$_2$RuSi$_4$Ti: C, 52.34; H, 5.90; N, 5.23. Found: C, 52.15; H, 6.22; N, 4.95.

(2) General Procedure for the Synthesis of the Heterodinuclear Complexes [MeSi{SiMe$_2$N(*p*-tol)}$_3$M−M′(CO)$_2$Cp] (M = Zr, Hf; M′ = Fe, Ru). To a mixture of solid [MeSi{SiMe$_2$N(*p*-tol)}$_3$MCl] (1.00 mmol) and 1.02 mmol of solid K[M′Cp(CO)$_2$] was slowly added 30 mL of toluene, which was precooled at −60 °C. The reaction mixture was stirred, warmed to ambient temperature over a period of 10 h, and stirred at 30 °C for another 24 h. The solvent was subsequently removed in vacuo, the residue was extracted with 40 mL of pentane, and the

(14) Casey, C. P.; Jordan, R. F.; Rheingold, A. L. *J. Am. Chem. Soc.* **1983**, *105*, 665.

(15) Casey, C. P.; Jordan, R. F.; Rheingold, A. L. *Organometallics* **1984**, *3*, 504.

(16) Casey, C. P.; Palermo, R. E.; Jordan, R. F. *J. Am. Chem. Soc.* **1985**, *107*, 4597.

(17) Casey, C. P.; Palermo, R. E. *J. Am. Chem. Soc.* **1986**, *108*, 549.

(18) Casey, C. P. *J. Organomet. Chem.* **1990**, *400*, 205.

(19) Sartain, W. S.; Selegue, J. P. *J. Am. Chem. Soc.* **1985**, *107*, 5818.

(20) Sartain, W. S.; Selegue, J. P. *Organometallics* **1987**, *6*, 1812.

(21) Sartain, W. S.; Selegue, J. P. *Organometallics* **1989**, *8*, 2153.

(22) Selent, D.; Beckhaus, R.; Pickardt, J. *Organometallics* **1993**, *12*, 2857.

(23) Gade, L. H.; Mahr, N. *J. Chem. Soc., Dalton Trans.* **1993**, 489.

(24) Gade, L. H.; Becker, C.; Lauher, J. W. *Inorg. Chem.* **1993**, *32*, 2308.

(25) Memmler, H.; Gade, L. H.; Lauher, J. W. *Inorg. Chem.* **1994**, *33*, 3064.

(26) Schubart, M.; Findeis, B.; Gade, L. H.; Li, W.-S.; McPartlin, M. *Chem. Ber.* **1995**, *128*, 329.

(27) Friedrich, S.; Gade, L. H.; Edwards, A. J.; McPartlin, M. *Chem. Ber* **1993**, *126*, 1797.

(28) Findeis, B.; Schubart, M.; Gade, L. H.; Möller, F.; Scowen, I. J.; McPartlin, M. *J. Chem. Soc., Dalton Trans.* **1996**, 125.

(29) Friedrich, S.; Memmler, H.; Gade, L. H.; Li, W.-S.; McPartlin, M. *Angew. Chem., Int. Ed. Engl.* **1994**, *33*, 676.

(30) Friedrich, S.; Memmler, H.; Gade, L. H.; Li, W.-S.; Scowen, I. J.; McPartlin, M.; Housecroft, C. E. *Inorg. Chem.* **1996**, *35*, 2433.

(31) Jansen, G.; Schubart, M.; Findeis, B.; Gade, L. H.; Scowen, I. J.; McPartlin, M. *J. Am. Chem. Soc.* **1998**, *120*, 7239.

(32) Findeis, B.; Schubart, M.; Platzek, C.; Gade, L. H.; Scowen, I. J.; McPartlin, M. *Chem. Commun.* **1996**, 219.

(33) Fabre, S.; Findeis, B.; Trösch, D. J. M.; Gade, L. H.; Scowen, I. J.; McPartlin, M. *Chem. Commun.* **1999**, 577.

(34) Brookhart, M.; Studabaker, W. B.; Husk, R. *Organometallics* **1987**, *6*, 1141.

extract was filtered. The filtrate was concentrated to ca. 5 mL and stored at −30 °C. Compounds **5**−**8** were obtained as yellow crystalline solids.

(a) [MeSi{SiMe₂N(p-tol)}₃Zr−Fe(CO)₂Cp] (5). Yield: 537 mg (67%). ¹H NMR (C₆D₆): δ = 0.13 (s, 3H, SiCH₃), 0.44 (s, 18H, Si(CH₃)₂), 2.16 (s, 9H, CH₃C₆H₄), 3.45 (s, 5H, C₅H₅), 7.16 (d, 6H, $^3J_{HH}$ = 8.1 Hz, H², H⁶), 7.38 (d, 6H, H³, H⁵). ¹³C{¹H} NMR (C₆D₆): δ = −15.4 (SiCH₃), 1.8 (Si(CH₃)₂), 20.8 (CH₃C₆H₄), 83.7 (C₅H₅), 116.9 (C², C⁶), 130.1 (C³, C⁵), 132.3 (C⁴), 146.4 (C¹), 213.5 (CO). ²⁹Si{¹H} NMR (C₆D₆): δ = −5.4 (Si(CH₃)₂), −98.4 (SiCH₃). IR (toluene): ν(CO) 1961, 1910 cm⁻¹. Anal. Calcd for C₃₅H₄₇FeN₃O₂Si₄Zr: C, 52.47; H, 5.91; N, 5.24. Found: C, 52.64; H, 5.97; N, 5.16.

(b) [MeSi{SiMe₂N(p-tol)}₃Zr−Ru(CO)₂Cp] (6). Yield: 635 mg (75%). ¹H NMR (C₆D₆): δ = 0.16 (s, 3H, SiCH₃), 0.49 (s, 18H, Si(CH₃)₂), 2.16 (s, 9 H, CH₃C₆H₄), 4.00 (s, 5 H, C₅H₅), 7.16 (d, 6H, $^3J_{HH}$ = 8.0 Hz, H², H⁶), 7.34 (d, 6H, H³, H⁵). ¹³C{¹H} NMR (C₆D₆): δ = −15.4 (SiCH₃), 1.8 (Si(CH₃)₂), 20.8 (CH₃C₆H₄), 86.5 (C₅H₅), 116.9 (C², C⁶), 130.1 (C³, C⁵), 132. 3 (C⁴), 145.4 (C¹), 203.2 (CO). ²⁹Si{¹H} NMR (C₆D₆): δ = −5.2 (Si(CH₃)₂), −98.7 (SiCH₃). IR (toluene): ν(CO) 1986, 1932 cm⁻¹. Anal. Calcd for C₃₅H₄₇N₃O₂RuSi₄Zr: C, 49.67; H, 5.60; N, 4.96. Found: C, 49.72; H, 5.38; N, 4.85.

(c) [MeSi{SiMe₂N(p-tol)}₃Hf−Fe(CO)₂Cp] (7). Yield: 613 mg (69%). ¹H NMR (C₆D₆): δ = 0.15 (s, 3H, SiCH₃), 0.46 (s, 18H, Si(CH₃)₂), 2.16 (s, 9H, CH₃C₆H₄), 3.55 (s, 5H, C₅H₅), 7.15 (d, 6H, $^3J_{HH}$ = 7.7 Hz, H², H⁶), 7.36 (d, 6H, H³, H⁵). ¹³C{¹H} NMR (C₆D₆): δ = −15.4 (SiCH₃), 2.3 (Si(CH₃)₂), 20.9 (CH₃C₆H₄), 83.4 (C₅H₅), 128.6 (C², C⁶), 130.2 (C³, C⁵), 132.4 (C⁴), 145.7 (C¹), 211.3 (CO). ²⁹Si{¹H} NMR (C₆D₆): δ = −5.4 (Si(CH₃)₂), −98.4 (SiCH₃). IR (toluene): ν(CO) 1969, 1915 cm⁻¹. Anal. Calcd for C₃₅H₄₇FeHfN₃O₂Si₄: C, 47.32; H, 5.33; N, 4.73. Found: C, 47.51; H, 5.38; N, 4.82.

(d) [MeSi{SiMe₂N(p-tol)}₃Hf−Ru(CO)₂Cp] (8). Yield: 570 mg (61%). ¹H NMR (C₆D₆): δ = 0.22 (s, 3H, SiCH₃), 0.49 (s, 18H, Si(CH₃)₂), 2.16 (s, 9H, CH₃C₆H₄), 3.98 (s, 5H, C₅H₅), 7.17 (d, 6 H, $^3J_{HH}$ = 7.8 Hz, H², H⁶), 7.33 (d, 6H, H³, H⁵). ¹³C{¹H} NMR (C₆D₆): δ = −15.3 (SiCH₃), 1.9 (Si(CH₃)₂), 20.7 (CH₃C₆H₄), 85.9 (C₅H₅), 117.3 (C², C⁶), 130.8 (C³, C⁵), 132. 9 (C⁴), 143.2 (C¹), 202.8 (CO). ²⁹Si{¹H} NMR (C₆D₆): δ = −4.7 (Si(CH₃)₂), −100.1 (SiCH₃). IR (toluene): ν(CO) 1987, 1933 cm⁻¹. Anal. Calcd for C₃₅H₄₇HfN₃O₂RuSi₄: C, 45.02; H, 5.07; N, 4.50. Found: C, 45.13; H, 5.19; N, 4.61.

(3) General Procedure for the Synthesis of MeSi{SiMe₂N(2-FC₆H₄)}₃Ti−M′(CO)₂Cp (M′ = Fe, Ru). To a mixture of solid [MeSi{SiMe₂N(2-FC₆H₄)}₃TiBr] (**2a**, 505 mg = 0.75 mmol) and 0.76 mmol of solid K[M′Cp(CO)₂] was slowly added 20 mL of toluene, which was precooled at −60 °C. The reaction mixture was stirred, warmed to ambient temperature over a period of 10 h, and stirred at 30 °C for another 24 h. The solvent was subsequently removed in vacuo, the residue was extracted with 20 mL of pentane, and the extract was filtered. The filtrate was concentrated to ca. 5 mL and stored at −30 °C. Compounds **9** and **10** were obtained as yellow crystalline solids.

(a) [MeSi{SiMe₂N(2-FC₆H₄)}₃Ti−Fe(CO)₂Cp] (9). Yield: 260 mg (45%). Mp: 96 °C dec. ¹H NMR (C₆D₆): δ = 0.02 (s, 3H, SiCH₃), 0.27, 0.29, 0.33, 0.35, 0.39, 0.43, 0.46, 0.47, 0.58, 0.60 (s, 18H, Si(CH₃)₂), 3.45, 3.63 (s, 5H, C₅H₅), 6.78−8.02 (m, 12H, aromatic protons). ¹³C{¹H} NMR (C₆D₆): δ = −14.5, −14.4 (SiCH₃), 1.0, 1.3, 1.7, 2.0, 2.2, 2.6, 3.0, 3.1 (Si(CH₃)₂), 84.9, 85.1 (C₅H₅), 115.5 (m, C³), 124.5 (m, C⁴,⁶), 130.4 (m, C⁵), 141.0 (m, C¹), 157.2 (d, $^1J_{FC}$ = 241 Hz, C²), 201.8 (CO). ²⁹Si{¹H} NMR (C₆D₆): δ = 0.3, 1.7 (Si(CH₃)₂), −88.7, −89.6 (SiCH₃). IR (toluene): ν(CO) 1980, 1932 cm⁻¹. Anal. Calcd for C₃₂H₃₈F₃FeN₃O₂Si₄Ti: C, 49.93; H, 4.98; N, 5.46. Found: C, 49.25; H, 5.27; N, 4.90.

(b) [MeSi{SiMe₂N(2-FC₆H₄)}₃Ti−Ru(CO)₂Cp] (10). Yield: 318 mg (52%). Mp: 76 °C dec. ¹H NMR (C₆D₆): δ = 0.08 (s, 3H, SiCH₃), 0.33, 0.35, 0.38, 0.41, 0.47, 0.49, 0.57, 0.59, 0.60, 0.74, 0.81 (s, 18H, Si(CH₃)₂), 4.07, 4.24 (s, 5H, C₅H₅), 6.75−8.00 (m, 12 H, aromatic protons). ¹³C{¹H} NMR (C₆D₆): δ = −14.3, −14.0 (SiCH₃), 0.6, 1.3, 1.7, 2.4, 2.8, 3.5, 3.7 (Si(CH₃)₂), 86.9, 87.0 (C₅H₅), 116.3 (m, C³), 124.3 (m, C⁴,⁶), 129.8 (C⁵), 139.3 (m, C¹), 156.5 (d, $^1J_{FC}$ = 242 Hz, C²), 201.8 (CO). ¹⁹F{¹H} NMR (C₆D₆, 295 K): δ = −116.7, −117.1. ²⁹Si{¹H} NMR (C₆D₆): δ = 0.3, 2.9 (Si(CH₃)₂), −85.6, −89.1 (SiCH₃). IR (toluene): ν(CO) 1997, 1940 cm⁻¹. Anal. Calcd for C₃₂H₃₈F₃RuN₃O₂Si₄Ti: C, 47.16; H, 4.70; N, 5.16. Found: C, 47.10; H, 4.64; N, 4.93.

(4) General Procedure for the Synthesis of the Heterodinuclear Complexes [MeSi{SiMe₂N(2-FC₆H₄)}₃M−M′(CO)₂Cp] (M = Zr, Hf; M′ = Fe, Ru). To a mixture of solid [MeSi{SiMe₂N(2-FC₆H₄)}₃-MCl] (1.00 mmol) and 1.02 mmol of solid K[M′Cp(CO)₂] was slowly added 30 mL of toluene, which was precooled at −60 °C. The reaction mixture was stirred, warmed to ambient temperature over a period of 10 h, and stirred at 30 °C for another 24 h. The solvent was subsequently removed in vacuo, the residue was extracted with 40 mL of pentane, and the extract was filtered. The filtrate was concentrated to ca. 5 mL and stored at −30 °C. Compounds **11**−**14** were obtained as yellow crystalline solids.

(a) [MeSi{SiMe₂N(2-FC₆H₄)}₃Zr−Fe(CO)₂Cp] (11). Yield: 382 mg (47%). Mp: 99 °C dec. ¹H NMR (C₆D₆): δ = 0.14 (s, 3H, SiCH₃), 0.44 (s, 18H, Si(CH₃)₂), 3.52 (s, 5H, C₅H₅), 6.71−7.57 (m, 12 H, aromatic protons). ¹³C{¹H} NMR (C₆D₆): δ = −15.8 (SiCH₃), 1.5 (Si(CH₃)₂), 83.5 (C₅H₅), 116.2 (d, $^3J_{FC}$ = 21 Hz, C³), 121.7 (m, C⁶), 124.4 (m, C⁴), 130.5 (C⁵), 137.5 (d, $^2J_{FC}$ = 15 Hz, C¹), 158.3 (d, $^1J_{FC}$ = 241 Hz, C²), 212.3 (CO). ¹⁹F{¹H} NMR (C₆D₆): δ = −119.1. ²⁹Si{¹H} NMR (C₆D₆): δ = −4.9 (Si(CH₃)₂), −99.7 (SiCH₃). IR (toluene): ν(CO) 1968, 1914 cm⁻¹. Anal. Calcd for C₃₂H₃₈F₃FeN₃O₂Si₄Zr: C, 47.27; H, 4.71; N, 5.17. Found: C, 47.35; H, 4.79; N, 5.32.

(b) MeSi{SiMe₂N(2-FC₆H₄)}₃Zr−Ru(CO)₂Cp (12). Yield: 378 mg (44%). Mp: 101 °C dec. ¹H NMR (C₆D₆): δ = 0.12 (s, 3H, SiCH₃), 0.46 (s, 18H, Si(CH₃)₂), 4.06 (s, 5H, C₅H₅), 6.72−7.54 (m, 12H, aromatic protons). ¹³C{¹H} NMR (C₆D₆): δ = −15.7 (SiCH₃), 1.4 (Si(CH₃)₂), 86.0 (C₅H₅), 116.2 (d, $^3J_{FC}$ = 22.0 Hz, C³), 124.0 (m, C⁴), 125.3 (m, C⁶), 130.1 (C⁵), 136.7 (d, $^1J_{FC}$ = 15.0 Hz, C¹), 158.0 (d, $^1J_{FC}$ = 225.0 Hz, C²), 201.9 (CO). ¹⁹F{¹H} NMR (C₆D₆, 295 K): δ = −119.2. ²⁹Si{¹H} NMR (C₆D₆): δ = −4.5 (Si(CH₃)₂), −99.2 (SiCH₃). IR (toluene): ν(CO) 1974, 1929 cm⁻¹. Anal. Calcd for C₃₂H₃₈F₃N₃O₂RuSi₄Zr: C, 44.78; H, 4.46; N, 4.90. Found: C, 44.83; H 4.59; N, 4.82.

(c) MeSi{SiMe₂N(2-FC₆H₄)}₃Hf−Fe(CO)₂Cp (13). Yield: 441 mg (49%). ¹H NMR (C₆D₆): δ = 0.17 (s, 3H, SiCH₃), 0.47 (s, 18 H, Si(CH₃)₂), 3.48 (s, 5H, C₅H₅), 6.54−7.55 (m, 12H, aromatic protons). ¹³C{¹H} NMR (C₆D₆): δ = −14.8 (SiCH₃), 2.6 (Si(CH₃)₂), 83.0 (C₅H₅), 113.9 (m, C³), 123.5 (m, C⁴), 124.4 (C⁶), 125.6 (C⁵), 139.6 (C¹), 159.3 (d, $^1J_{FC}$ = 237 Hz, C²), 212.4 (CO). ¹⁹F{¹H} NMR (C₆D₆): δ = −118.9. ²⁹Si{¹H} NMR (C₆D₆): δ = −7.3 (Si(CH₃)₂), −100.2 (SiCH₃). IR (toluene): ν(CO) 1971, 1917 cm⁻¹. Anal. Calcd for C₃₂H₃₈F₃FeHfN₃O₂Si₄: C, 42.69; H, 4.25; N, 4.67. Found: C, 42.78; H, 4.39; N, 4.74.

(d) [MeSi{SiMe₂N(2-FC₆H₄)}₃Hf−Ru(CO)₂Cp] (14). Yield: 435 mg (46%). ¹H NMR (C₆D₆): δ = 0.12 (s, 3H, SiCH₃), 0.45 (s, 18H, Si(CH₃)₂), 4.06 (s, 5H, C₅H₅), 6.68−7.55 (m, 12H, aromatic protons). ¹³C{¹H} NMR (C₆D₆): δ = −15.6 (SiCH₃), 1.4 (Si(CH₃)₂), 86.1 (C₅H₅), 116.2 (d, $^3J_{FC}$ = 22 Hz, C³), 124.1 (d, $^4J_{FC}$ = 7 Hz, C⁴), 124.9 (C⁶), 130.2 (C⁵), 136.7 (d, $^2J_{FC}$ = 14 Hz, C¹), 158.1 (d, $^1J_{FC}$ = 240 Hz, C²), 202.0 (CO). ¹⁹F{¹H} NMR (C₆D₆): δ = −119.2. ²⁹Si{¹H} NMR (C₆D₆): δ = −4.3 (Si(CH₃)₂), −100.3 (SiCH₃). IR (toluene): ν(CO) 1979 s, 1934 cm⁻¹. Anal. Calcd for C₃₂H₃₈F₃HfN₃O₂RuSi₄: C, 40.65; H, 4.05; N, 4.44. Found: C, 40.89; H, 4.23; N, 4.52.

(5) General Procedure for the Preparation of [MeSi{SiMe₂NR}₃Ti-{η²-C(=NR′)M′Cp(CO)₂}] (R = p-tol, 2-C₆H₄; R′ = Me, p-tol; M′ = Fe, Ru). To a solution of 0.5 mmol of the heterodinuclear complex [MeSi{SiMe₂NR}₃Ti−M′Cp(CO)₂}] in 10 mL of toluene was added at room temperature an equimolar amount of the isonitrile. A change of color in the solution from yellow to orange immediately indicated the conversion of the starting material. All insertion products were isolated by removal of the solvent in vacuo and washing of the yellow solid residue with 1 mL of ice-cold pentane. Crystals of **17a** were grown by recrystallization from pentane at −30 °C.

(a) [MeSi{SiMe₂N(p-tol)}₃Ti{η²-C(=NMe)FeCp(CO)₂}] (15a). Yield: 380 mg (95%). ¹H NMR (C₆D₆): δ = 0.39 (s, 3H, SiCH₃), 0.57 (s, 18 H, Si(CH₃)₂), 2.19 (s, 9H, CH₃C₆H₄), 2.92 (s, 3H, NCH₃), 4.16 (s, 5H, C₅H₅), 6.72 (d, 6 H, $^3J_{HH}$ = 8.2 Hz, H², H⁶), 6.96 (d, 6H, H³, H⁵). ¹³C{¹H} NMR (C₆D₆): δ = −15.5 (SiCH₃), 2.5 (Si(CH₃)₂), 20.9 (CH₃C₆H₄), 41.8 (CH₃N), 88.4 (C₅H₅), 124.7 (C², C⁶), 129.5 (C⁴), 129.8 (C³, C⁵), 153.8 (C¹), 213.4 (CO), 277.3 (TiCNCH₃). ²⁹Si{¹H} NMR (C₆D₆): δ = −6.2 (Si(CH₃)₂), −98.5 (SiCH₃). IR (toluene): ν(CO) 2012, 1963 cm⁻¹. Anal. Calcd for C₃₇H₅₀FeN₄O₂Si₄Ti: C, 55.62; H, 6.32; N, 7.01. Found: C, 55.71; H, 6.39; N, 7.08.

(b) [MeSi{SiMe₂N(*p*-tol)}₃Ti{η²-C(=N{*p*-tol})FeCp(CO)₂}] (15b).
Yield: 416 mg (95%). ¹H NMR (C₆D₆): δ = 0.39 (s, 3H, SiCH₃),
0.58 (s, 18 H, Si(CH₃)₂), 2.10 (s, 3H C*H₃*C₆H₄NC), 2.16 (s, 3H,
C*H₃*C₆H₄), 4.12 (s, 5 H, C₅H₅), 6.58 (d, 6H, $^3J_{HH}$ = 8.2 Hz, H²,⁶,
TolNC), 6.81 (d, 6 H, H³,⁵, TolNC), 6.82 (d, 6 H, $^3J_{HH}$ = 8.2 Hz, H²,⁶,
Tol), 6.90 (d, 6 H, H³,⁵, Tol). ¹³C{¹H} NMR (C₆D₆): δ = −15.1 (SiCH₃),
2.5 (Si(CH₃)₂), 20.8, 21.0 (*C*H₃C₆H₄), 87.8 (C₅H₅), 122.2 (C²,⁶, TolNC),
125.0 (C²,⁶, Tol), 128.9 (C³,⁵, Tol), 129.2 (C³,⁵, Tol), 129.9 (C⁴, Tol),
130.1 (C⁴, TolNC), 149.6 (C¹, TolNC), 153.8 (C¹, Tol), 213.1 (CO),
287.3 (Ti*C*=NCH₃). ²⁹Si{¹H} NMR (C₆D₆): δ = −4.8 (Si(CH₃)₂),
−96.1 (SiCH₃). IR (toluene): ν(CO) 2015, 1977 cm⁻¹. Anal. Calcd
for C₄₃H₅₄FeN₄O₂Si₄Ti: C, 59.03; H, 6.22; N, 6.40. Found: C, 58.79;
H, 6.03; N, 6.31.

(c) [MeSi{SiMe₂N(2-FC₆H₄)}₃Ti{η²-C(=NMe)FeCp(CO)₂}] (16a).
Yield: 276 mg (68%). ¹H NMR (C₆D₆): δ = 0.37 (s, 3H, SiCH₃),
0.59 (s, 18H, Si(CH₃)₂), 2.91 (s, 3H, NCH₃), 4.15 (s, 5H, C₅H₅), 6.63−
7.01 (m, 12H, aromatic protons). ¹³C{¹H} NMR (C₆D₆): δ = −15.5
(SiCH₃), 1.9 (Si(CH₃)₂), 41.3 (CH₃N), 88.1 (C₅H₅), 115.5 (d, $^2J_{FC}$ =
21.6 Hz, C³,⁵, FC₆H₄), 121.7 (d, $^2J_{FC}$ = 7.0 Hz, C²,⁶, FC₆H₄), 124.2
(C⁴), 124.6 (C⁶), 143.7 (d, $^2J_{FC}$ = 14.1 Hz, C¹, FC₆H₄), 153.8 (d, $^1J_{FC}$
= 239.5 Hz, C²), 213.0 (CO), 274.7 (Ti*C*NCH₃). ²⁹Si{¹H} NMR
(C₆D₆): δ = −3.9 (Si(CH₃)₂), −96.9 (SiCH₃). IR (toluene): ν(CO)
2020, 1969 cm⁻¹. Anal. Calcd for C₃₄H₄₁F₃FeN₄O₂Si₄Ti: C, 50.37; H,
5.10; N, 6.91. Found: C, 49.71; H, 5.39; N, 7.08.

(d) [MeSi{SiMe₂N(2-FC₆H₄)}₃Ti{η²-C(=N{*p*-tol})FeCp(CO)₂}]
(16b). Yield: 333 mg (75%). ¹H NMR (C₆D₆): δ = 0.36 (s, 3H,
SiCH₃), 0.60 (s, 18H, Si(CH₃)₂), 2.06 (s, 3H, C*H₃*C₆H₄NC), 4.17 (s,
5H, C₅H₅), 6.58−6.85 (m, aromatic protons). ¹³C{¹H} NMR (C₆D₆):
δ = −15.1 (SiCH₃), 2.1 (Si(CH₃)₂), 21.1 (*C*H₃C₆H₄), 88.1 (C₅H₅), 115.5
(d, $^2J_{FC}$ = 21.6 Hz, C³,⁵, FC₆H₄), 121.9 (d, $^2J_{FC}$ = 6.5 Hz, C²,⁶, FC₆H₄),
122.3 (C²,⁶, TolNC), 124.0 (C⁴, FC₆H₄), 124.7 (C⁵, FC₆H₄) 129.1 (C³,⁵,
TolNC), 134.9 (C⁴, TolNC), 143.7 (C¹, FC₆H₄), 148.5 (C¹, TolNC),
156.5 (C², FC₆H₄), 212.8 (CO), 284.6 (Ti*C*=NCH₃). ²⁹Si{¹H} NMR
(C₆D₆): δ = −2.8 (Si(CH₃)₂), −95.7 (SiCH₃). IR (toluene): ν(CO)
2009, 1970 cm⁻¹. Anal. Calcd for C₄₀H₄₆F₃FeN₄O₂Si₄Ti: C, 54.11; H,
5.22; N, 6.31. Found: C, 53.71; H, 5.07; N, 6.89.

(e) [MeSi{SiMe₂N(*p*-tol)}₃Ti{η²-C(=NMe)RuCp(CO)₂}] (17a).
Yield: 342 mg (96%). ¹H NMR (C₆D₆): δ = 0.36 (s, 3H, SiCH₃),
0.59 (s, 18 H, Si(CH₃)₂), 2.19 (s, 9H, C*H₃*C₆H₄), 2.91 (s, 3H, NCH₃),
4.70 (s, 5H, C₅H₅), 6.72 (d, 6H, $^3J_{HH}$ = 8.0 Hz, H², H⁶), 7.00 (d, 6H,
H³, H⁵). ¹³C{¹H} NMR (C₆D₆): δ = −15.9 (SiCH₃), 2.4 (Si(CH₃)₂),
20.8 (*C*H₃C₆H₄), 42.6 (CH₃N), 91.2 (C₅H₅), 124.4 (C², C⁶), 129.0 (C⁴),
129.9 (C³, C⁵), 150.8 (C¹), 203.3 (CO), 267.3 (Ti*C*NCH₃). ²⁹Si{¹H}
NMR (C₆D₆): δ = −6.5 (Si(CH₃)₂), −98.9 (SiCH₃). IR (toluene):
ν(CO) 2018, 1971 cm⁻¹. Anal. Calcd for C₃₇H₅₀N₄O₂RuSi₄Ti: C, 52.76;
H, 5.98; N, 6.65. Found: C, 52.64; H, 5.91; N, 6.82.

(f) [MeSi{SiMe₂N(*p*-tol)}₃Ti{η²-C(=N{*p*-tol})RuCp(CO)₂}] (17b).
Yield: 405 mg (88%). ¹H NMR (C₆D₆): δ = 0.40 (s, 3H, SiCH₃),
0.58 (s, 18H, Si(CH₃)₂), 2.11 (s, 3H, C*H₃*C₆H₄NC), 2.16 (s, 9H,
C*H₃*C₆H₄), 4.68 (s, 5H, C₅H₅), 6.60 (d, 2H, $^3J_{HH}$ = 8.4 Hz, H²,⁶, TolNC),
6.80 (d, 2H, H³,⁵, TolNC), 6.82 (d, 6H, $^3J_{HH}$ = 8.2 Hz, H²,⁶, Tol), 6.89
(d, 6H, H³,⁵, Tol). ¹³C{¹H} NMR (C₆D₆): δ = −15.1 (SiCH₃), 2.5
(Si(CH₃)₂), 20.8, 21.0 (*C*H₃C₆H₄), 90.8 (C₅H₅), 122.3 (C²,⁶, TolNC),
125.0 (C²,⁶, Tol), 128.9 (C³,⁵, Tol), 129.2 (C³,⁵, Tol), 129.8 (C⁴, Tol),
134.5 (C⁴, TolNC), 150.3 (C¹, TolNC), 153.0 (C¹, Tol), 198.3 (CO),
276.0 (Ti*C*=NCH₃). ²⁹Si{¹H} NMR (C₆D₆): δ = −5.0 (Si(CH₃)₂),
−96.4 (SiCH₃). IR (toluene): ν(CO) 2025, 1980 cm⁻¹. Anal. Calcd
for C₄₃H₅₄RuN₄O₂Si₄Ti: C, 56.12; H, 5.91; N, 6.09. Found: C, 55.89;
H, 5.75; N, 5.89.

(g) [MeSi{SiMe₂N(2-FC₆H₄)}₃Ti{η²-C(=NMe)RuCp(CO)₂}] (18a).
Yield: 291 mg (68%). ¹H NMR (C₆D₆): δ = 0.38 (s, 3H, SiCH₃),
0.59 (s, 18H, Si(CH₃)₂), 2.90 (s, 3H, NCH₃), 4.68 (s, 5H, C₅H₅), 6.61−
7.00 (m, 12H, aromatic protons). ¹³C{¹H} NMR (C₆D₆): δ = −15.6
(SiCH₃), 1.8 (Si(CH₃)₂), 42.2 (CH₃N), 90.9 (C₅H₅), 115.5 (d, $^2J_{FC}$ =
21.9 Hz, C³,⁵, FC₆H₄), 121.6 (d, $^2J_{FC}$ = 6.9 Hz, C²,⁶, FC₆H₄), 124.6
(C⁴), 124.6 (C⁶), 143.9 (d, $^2J_{FC}$ = 14.1 Hz, C¹, FC₆H₄), 156.4 (d, $^1J_{FC}$
= 239.4 Hz, C²), 198.2 (CO), 265.2 (Ti*C*NCH₃). ²⁹Si{¹H} NMR
(C₆D₆): δ = −4.2 Si(CH₃)₂), −97.2 (SiCH₃). IR (toluene): ν(CO) 2030,
1970 cm⁻¹. Anal. Calcd for C₃₄H₄₁F₃N₄O₂RuSi₄Ti: C, 47.71; H, 4.83;
N, 6.55. Found: C, 46.89; H, 5.05; N, 6.39.

(h) [MeSi{SiMe₂N(2-FC₆H₄)}₃Ti{η²-C(=N{*p*-tol})RuCp(CO)₂}]
(18b). Yield: 350 mg (75%). ¹H NMR (C₆D₆): δ = 0.36 (s, 3H,
SiCH₃), 0.60 (s, 18H, Si(CH₃)₂), 2.07 (s, 3H, C*H₃*C₆H₄NC), 4.71 (s,
5H, C₅H₅), 6.58−6.86 (m, aromatic protons). ¹³C{¹H} NMR (C₆D₆):
δ = −15.3 (SiCH₃), 2.0 (Si(CH₃)₂), 21.0 (*C*H₃C₆H₄), 90.8 (C₅H₅), 115.4
(d, $^2J_{FC}$ = 21.6 Hz, C³,⁵, FC₆H₄), 121.8 (d, $^2J_{FC}$ = 6.5 Hz, C²,⁶, FC₆H₄),
122.2 (C²,⁶, TolNC), 123.9 (C⁴, FC₆H₄), 124.0 (C⁵, FC₆H₄), 129.0 (C³,⁵,
TolNC), 134.9 (C⁴, TolNC), 143.4 (C¹, FC₆H₄), 149.3 (C¹, TolNC),
156.4 (d, $^1J_{FC}$ = 239.3 Hz, C², FC₆H₄), 208.0 (CO), 274.3 (Ti*C*=NCH₃).
²⁹Si{¹H} NMR (C₆D₆): δ = −3.1 (Si(CH₃)₂), −96.0 (SiCH₃). IR
(toluene): ν(CO) = 2025, 1975 cm⁻¹. Anal. Calcd for C₃₄H₄₁F₃N₄O₂-
RuSi₄Ti: C, 47.71; H, 4.83; N, 6.55. Found: C, 46.89; H, 5.05; N,
6.39.

**(6) General Procedure for the Preparation of [MeSi{SiMe₂N(*p*-
tol)}₃M{η²-C(=NMe)M′Cp(CO)₂}] (M = Zr, Hf; M′ = Fe, Ru).**
The synthesis of compounds **19−22** was carried out under the same
conditions as described for the Ti−M complexes using 0.2 mmol of
the heterodinuclear complex. In all cases, analytically pure products
were obtained by removal of the solvent in vacuo and washing of the
light yellow solid residue with 1−2 mL of ice-cold pentane.

(a) [MeSi{SiMe₂N(*p*-tol)}₃Zr{η²-C(=NMe)FeCp(CO)₂}] (19).
Yield: 163 mg (97%). ¹H NMR (C₆D₆): δ = 0.36 (s, 3H, SiCH₃),
0.55 (s, 18H, Si(CH₃)₂), 2.18 (s, 9H, C*H₃*C₆H₄), 2.92 (s, 3H, NCH₃),
4.16 (s, 5H, C₅H₅), 6.75 (d, 6H, $^3J_{HH}$ = 8.1 Hz, H²,⁶), 6.96 (d, 6H,
H³,⁵). ¹³C{¹H} NMR (C₆D₆): δ = −16.7 (SiCH₃), 2.4 (Si(CH₃)₂), 20.8
(*C*H₃C₆H₄), 43.4 (CH₃N), 88.8 (C₅H₅), 124.9 (C²,⁶), 129.8 (C⁴), 129.9
(C³,⁵), 151.4 (C¹), 214.4 (CO), 289.3 (Zr*C*NCH₃). ²⁹Si{¹H} NMR
(C₆D₆): δ = −11.2 (Si(CH₃)₂), −106.2 (SiCH₃). IR (toluene): 3011
w, 2952 m, 2887 w, 2156 m, 2010 s, 1966 s, 1605 m, 1511 s, 1496 s,
1443 w, 1362 w, 1283 m, 1248 m, 1237 s, 1224 s, 935 m, 904 m, 892
m, 843 s, 814 m, 783 m, 703 w cm⁻¹. Anal. Calcd for C₃₇H₅₀FeN₄O₂-
Si₄Zr: C, 52.76; H, 5.98; N, 6.65. Found: C, 52.64; H, 5.91; N, 6.82.

(b) [MeSi{SiMe₂N(*p*-tol)}₃Zr{η²-C(=NMe)RuCp(CO)₂}] (20).
Yield: 150 mg (95%). ¹H NMR (C₆D₆): δ = 0.36 (s, 3H, SiCH₃),
0.55 (s, 18 H, Si(CH₃)₂), 2.18 (s, 9H, C*H₃*C₆H₄), 2.87 (s, 3H, NCH₃),
4.70 (s, 5H, C₅H₅), 6.73 (d, 6H, $^3J_{HH}$ = 8.2 Hz, H²,⁶), 6.95 (d, 6H,
H³,⁵). ¹³C{¹H} NMR (C₆D₆): δ = −16.8 (SiCH₃), 2.4 (Si(CH₃)₂), 20.7
(*C*H₃C₆H₄), 44.5 (CH₃N), 91.8 (C₅H₅), 124.9 (C²,⁶), 129.6 (C⁴), 129.7
(C³,⁵), 151.4 (C¹), 199.5 (CO), 278.4 (Zr*C*NCH₃). ²⁹Si{¹H} NMR
(C₆D₆): δ = −11.4 (Si(CH₃)₂), −97.4 (SiCH₃). IR (toluene): 3021 w,
2962 w, 2928 w, 2042 s, 1975 s, 1609 m, 1514 m, 1502 s, 1289 m,
1253 s, 1242 s, 1231 s, 939 m, 912 s, 854 s, 789 m, 743 m, 709 w,
687 w cm⁻¹. Anal. Calcd for C₃₇H₅₀N₄O₂RuSi₄Zr: C, 50.08; H, 5.68;
N, 6.31. Found: C, 50.31; H, 5.74; N, 6.46.

(c) [MeSi{SiMe₂N(*p*-tol)}₃Hf{η²-C(=NMe)FeCp(CO)₂}] (21).
Yield: 162 mg (94%). ¹H NMR (C₆D₆): δ = 0.38 (s, 3H, SiCH₃),
0.55 (s, 18H, Si(CH₃)₂), 2.20 (s, 9H, C*H₃*C₆H₄), 2.95 (s, 3H, NCH₃),
4.14 (s, 5H, C₅H₅), 6.78 (d, 6H, $^3J_{HH}$ = 8.1 Hz, H²,⁶), 6.97 (d, 6H,
H³,⁵). ¹³C{¹H} NMR (C₆D₆): δ = −17.1 (SiCH₃), 2.4 (Si(CH₃)₂), 20.7
(*C*H₃C₆H₄), 44.0 (CH₃N), 88.8 (C₅H₅), 125.5 (C²,⁶), 129.8 (C³,⁵), 130.0
(C⁴), 150.8 (C¹), 214.3 (CO), 303.8 (Zr*C*NCH₃). ²⁹Si{¹H} NMR
(C₆D₆): δ = −8.9 (Si(CH₃)₂), −109.1 (SiCH₃). IR (toluene): 3011 w,
2951 m, 2890 w, 2858 w, 2004 s, 1961 s, 1603 m, 1508 s, 1497 s,
1364 w, 1279 m, 1238 s, 1219 s, 1116 m, 934 m, 883 m, 852 s, 781
s, 706 m, 648 w cm⁻¹. Anal. Calcd for C₃₇H₅₀FeHfN₄O₂Si₄: C, 47.81;
H, 5.42; N, 6.03. Found: C, 48.12; H, 5.53; N, 6.16.

(d) [MeSi{SiMe₂N(*p*-tol)}₃Hf{η²-C(=NMe)RuCp(CO)₂}] (22).
Yield: 190 mg (97%). ¹H NMR (C₆D₆): δ = 0.35 (s, 3H, SiCH₃),
0.55 (s, 18H, Si(CH₃)₂), 2.19 (s, 9H, C*H₃*C₆H₄), 2.90 (s, 3H, NCH₃),
4.68 (s, 5H, C₅H₅), 6.78 (d, 6 H, $^3J_{HH}$ = 10.0 Hz, H²,⁶), 6.96 (d, 6H,
H³,⁵). ¹³C{¹H} NMR (C₆D₆): δ = −17.2 (SiCH₃), 2.3 (Si(CH₃)₂), 20.7
(*C*H₃C₆H₄), 45.2 (CH₃N), 91.9 (C₅H₅), 125.5 (C²,⁶), 129.6 (C⁴), 130.0
(C³,⁵), 150.8 (C¹), 199.6 (CO), 292.4 (Hf*C*NCH₃). IR (toluene): ν(CO)
= 2019, 1971 cm⁻¹. Anal. Calcd for C₃₇H₅₀RuHfN₄O₂Si₄: C, 45.59;
H, 5.17; N, 5.75. Found: C, 45.28; H, 5.02; N, 5.99.

(7) General Procedure for the Reaction of 6 with Sulfoxides. To
a solution of [MeSi(SiMe₂NTol)₃Zr−RuCp(CO)₂] (**6**) (400 mg = 0.47
mmol) in 10 mL of toluene was added 0.47 mmol of sulfoxide at −40
°C, and the reaction mixture was then warmed to ambient temperature.
Removal of the solvent in vacuo at 0 °C and washing of the residue
with cold pentane yielded compounds **23a−d** as yellow powders in

nearly quantitative yield. Addition of a second equivalent of sulfoxide to **23a−c** led to the immediate and quantitative conversion to **24a−c** (¹H NMR). After reduction of the solvent volume to ca. 5 mL and addition of 5 mL of pentane, the solution was stored at −35 °C. The yellow solid product crystallized over a period of several days.

(a) [MeSi{SiMe₂N(p-tol)}₃Zr(μ-O₂C)Ru(CO){SMe₂}Cp] (23a). Yield: 143 mg (33%). ¹H NMR (C₆D₆): δ = 0.33 (s, 3H, CH₃Si), 0.52−0.54 (s, 18H, Si(CH₃)₂), 1.54 (s, br, 6H, S(CH₃)₂), 2.18 (s, 9H, C₆H₄CH₃), 4.31 (s, 5H, C₅H₅), 6.97−7.01−7.03−7.08 (dd, 12H, Tol) ¹³C{¹H} NMR (C₆D₆): δ = −15.9 (CH₃Si), 2.3, 2.5 (Si(CH₃)₂), 20.9 (C₆H₄CH₃), 27.8 (S(CH₃)₂), 87.0 (C₅H₅), 126.6 (C²,⁶, Tol), 129.7 (C³,⁵, Tol), 130.5 (C⁴, Tol), 148.4 (C¹, Tol), 204.1 (CO), 235.4 (CO₂). IR (benzene): ν(CO) 1957 cm⁻¹. Anal. Calcd for C₃₇H₅₃N₃O₃RuSSi₄Zr: C, 48.07; H, 5.78; N, 4.54. Found: C, 48.23; H, 5.29; N, 4.51.

(b) [MeSi{SiMe₂N(p-tol)}₃Zr(μ-O₂C)Ru(CO){S(Me)Ph}Cp] (23b). Yield: 180 mg (39%). ¹H NMR (C₆D₆): δ = 0.35 (s, 3H, CH₃Si), 0.56−0.59 (s, 18H, Si(CH₃)₂), 2.08 (s, 3H, S(CH₃)Ph), 2.15 (s, 9H, C₆H₄CH₃), 4.27 (s, 5H, C₅H₅), 6.8−7.2 (m, 17H, Tol and S(CH₃)*Ph*). ¹³C{¹H} NMR (C₆D₆): δ = −15.5 (CH₃Si), 2.5, 2.7 (Si(CH₃)₂), 27.5 (C₆H₄CH₃), 30.3 (S(CH₃)Ph), 87.2 (C₅H₅), 126.9 (C²,⁶, Tol), 129.5 (C³,⁵, Tol), 130.4 (C⁴, Tol), 149.5 (C¹, Tol), 129.8, 129.1, 124.6 (C²′⁻⁶′, S(CH₃)Ph), 141.1 (C¹′, S(CH₃)Ph), 204.8 (CO), 232.0 (CO₂). IR (benzene): ν(CO) 1947 cm⁻¹. Anal. Calcd for C₄₂H₅₅N₃O₃RuSSi₄Zr: C, 51.13; H, 5.62; N, 4.26. Found: C, 51.02; H, 5.37; N, 4.55.

(c) [MeSi{SiMe₂N(p-tol)}₃Zr(μ-O₂C)Ru(CO){S(CH₂)₄}Cp] (23c). Yield: 125 mg (28%). ¹H NMR (C₆D₆): δ = 0.32 (s, 3H, CH₃Si), 0.53, 0.54 (s, 18H, Si(CH₃)₂), 1.40 and 2.00−2.20 (m, br, 8H, S(C₄H₈)), 2.19 (s, 9H, C₆H₄CH₃), 4.39 (s, 5H, C₅H₅), 6.90−7.15 (m, 12H, Tol). ¹³C{¹H} NMR (C₆D₆): δ = −15.9 (CH₃Si), 1.8, 2.4 (Si(CH₃)₂), 21.0 (C₆H₄CH₃), 30.0, 43.1 (S(C₄H₈)), 86.9 (C₅H₅), 126.5 (C²,⁶, Tol), 129.6 (C³,⁵, Tol), 130.4 (C⁴, Tol), 148.5 (C¹, Tol), 204.3 (CO), 231.3 (CO₂). IR (benzene): ν(CO) 1940 cm⁻¹. Anal. Calcd for C₃₉H₅₅N₃O₃RuSSi₄-Zr: C, 49.28; H, 5.83; N, 4.42. Found: C, 48.77; H, 5.63; N, 4.39.

(d) [MeSi{SiMe₂N(p-tol)}₃Zr(μ-O₂C)Ru(CO){S(CH₂Ph)₂}Cp] (23d). Yield: 105 mg (21%). ¹H NMR (C₆D₆): δ = 0.35 (s, 3H, C*H₃*Si), 0.56, 0.58 (s, 18H, Si(CH₃)₂), 1.97 (s, 9H, C₆H₄CH₃), 3.5 (s, 4H, S(C*H₂*C₆H₅)₂), 4.09 (s, 5H, C₅*H₅*), 6.99−7.21 (m, 22H, C₆*H₄*CH₃ and S(CH₂C₆*H₅*)₂). ¹³C{¹H} NMR (C₆D₆): δ = −15.9 (C*H₃*Si), 2.3, 2.6 (Si(CH₃)₂), 20.8 (C₆H₄CH₃), 44.3 [S(C*H₂*C₆H₅)₂], 86.5 (C₅H₅), 126.4 (C²C,⁶ C₆H₄CH₃), 130.1 (C³, C,⁵ C₆H₄CH₃), 130.9 (C,⁴ C₆H₄CH₃), 148.3 (C¹, C₆H₄CH₃), 130.8, 129.4, 128.6 (S(CH₂C₆H₅)₂), 204.6 (*C*O), 236.8 (*C*O₂). IR (benzene): ν(CO): 1960 cm⁻¹. Anal. Calcd for C₄₉H₆₁N₃O₃-RuSSi₄Zr: C, 54.66; H, 5.71; N, 3.90. Found: C, 54.26; H, 5.53; N, 4.39.

(e) [MeSi{SiMe₂N(p-tol)}₃(Me₂SO)Zr(μ-O₂C)Ru(CO){SMe₂}Cp] (24a). Yield: 348 mg (74%). ¹H NMR (C₆D₆): δ = 0.38 (s, 3H, CH₃Si), 0.56, 0.65 (s, 18H, Si(CH₃)₂), 1.66 (s, 6H, OS(CH₃)₂), 1.72 (s, br, 6H, S(CH₃)₂), 2.24 (s, 9H, C₆H₄C*H₃*), 4.48 (s, 5H, C₅H₅), 7.00−7.17 (m, 12H, Tol). ¹³C{¹H} NMR (C₆D₆): δ = −14.5 (CH₃Si), 2.6, 3.2 (Si-(CH₃)₂), 21.1 (C₆H₄CH₃), 26.0 (S(CH₃)₂), 39.5 (OS(CH₃)₂), 86.8 (C₅H₅), 127.8 (C²,⁶, Tol), 128.9 (C³,⁵, Tol), 128.9 (C⁴, Tol), 152.3 (C¹, Tol), 207.4 (CO), 225.1 (CO₂). IR (benzene): ν(CO) 1924 cm⁻¹. Anal. Calcd for C₃₉H₅₉N₃O₄RuS₂Si₄Zr: C, 46.72; H, 5.93; N, 4.19. Found: C, 45.96; H, 5.74; N, 4.07.

(f) [MeSi{SiMe₂N(p-tol)}₃{Me(Ph)SO}Zr(μ-O₂C)Ru(CO){S(Ph)-Me}Cp] (24b). Yield: 217 mg (41%). ¹H NMR (C₆D₆): δ = 0.39 (s, 3H, CH₃Si), 0.60, 0.64 (s, 18H, Si(CH₃)₂), 1.98 (s, br, 3H, OS(CH₃)-Ph)), 2.17 (s, 9H, C₆H₄CH₃), 2.43 (s, 3H, S(C*H₃*)Ph), 4.37 (s, 5H, C₅H₅), 6.8−7.4 (m, 17H, Tol and S(CH₃)*Ph*). ¹³C{¹H} NMR (C₆D₆): δ = −14.5 (CH₃Si), 2.8, 2.9 (Si(CH₃)₂), 21.1 (OS(CH₃)Ph)), 27.8 (C₆H₄CH₃), 42.8 (S(C*H₃*)Ph), 87.5 (C₅H₅), 127.8 (C²,⁶, Tol), 128.9 (C³,⁵, Tol), 129.1 (C⁴, Tol), 151.8 (C¹, Tol), 124.1, 128.2, 129.0, 129.2, 129.8, 130.8 (C²′⁻⁶′ and C²″⁻⁶″, OS(CH₃)*Ph* and S(CH₃)*Ph*), 142.1 (C¹′, S(CH₃)Ph), 145.5 (C¹″, OS(CH₃)Ph), 206.9 (CO), 225.6 (CO₂). IR (benzene): ν(CO) 1937 cm⁻¹. Anal. Calcd for C₄₉H₆₃N₃O₄RuS₂Si₄Zr: C, 52.23; H, 5.64; N, 3.73. Found: C, 52.14; H, 5.23; N, 4.09.

(g) [MeSi{SiMe₂N(p-tol)}₃}{(CH₂)₄SO}Zr(μ-O₂C)Ru(CO)-{S(CH₂)₄}Cp] (24c). Yield: 173 mg (35%). ¹H NMR (C₆D₆): δ = 0.36 (s, 3H, CH₃Si), 0.56−0.61 (s, 18H, Si(CH₃)₂), 1.40, 2.20 (m, br, 16H, S(C₄H₈) and OS(C₄H₈)), 2.26 (s, 9H, C₆H₄C*H₃*), 4.62 (s, 5H, C₅H₅), 7.01−7.15 (m, 12H, Tol). ¹³C{¹H} NMR (C₆D₆): δ = −14.7

(CH₃Si), 2.6, 3.1 (Si(CH₃)₂), 21.1 (C₆H₄CH₃), 25.9, 52.6 (OS(C₄H₈)), 30.0 (S(C₄H₈)), 87.4 (C₅H₅), 127.7 (C²,⁶, Tol), 128.71 (C³,⁵, Tol), 152.2 (C¹, Tol), 207.2 (CO), 225.0 (CO₂). IR (benzene): ν(CO) 1932 cm⁻¹. Anal. Calcd for C₄₃H₆₃N₃O₄RuS₂Si₄Zr: C, 48.97; H, 6.02; N, 3.98. Found: C, 48.43; H, 5.88; N, 4.27.

(8) X-ray Crystallographic Study of 3, 4, 5, 9, 17a, and 24a. (a) Data Collection for 3, 4, 5, 9, 17a, and 24a. Crystals of **3**, **4**, **5**, **9**, **17a**, and **24a** were mounted on a quartz fiber in Lindemann capillaries under argon and in an inert oil. X-ray intensity data were collected with graphite-monochromated radiation, on a Siemens P4 four-circle diffractometer for **4**, **9**, **17a**, and **24a** and on a Philips PW1100 four-circle diffractometer for **3** and **5**. Details of data collection and refinement and crystal data are listed in Table 1. Lorentz−polarization and absorption corrections were applied to the data of all of the compounds.

(b) Structure Solution and Refinement for 3, 4, 5, 9, 17a, and 24a. For the isomorphous crystals of **3**−**5**, the positions of the metal atoms were deduced from Patterson syntheses, and for **9**, **17a**, and **24a**, the positions of most of the non-hydrogen atoms were located by direct methods.[35,36] The remaining non-hydrogen atoms were revealed from subsequent difference Fourier syntheses. The crystals of **9** diffracted poorly at high angles, and data in the limited θ range of 2.14−18° were used in structure solution and refinement. The weak diffraction may be related to the random distribution, throughout the crystal, of the two conformers (Figure 3) detected in the NMR spectrum of **9**. The presence of two conformers, which are virtually superimposed in the structure analysis, is indicated by the disorder of the ortho fluorine atoms of the two phenyl rings over the two alternative sites [F(12)/F(16) and F(32)/F(36) 60/40% occupancy] and by relatively high displacement parameters for some phenyl carbon atoms; the possibility of a similar disorder for F(22) may be ruled out not only by the lack of any significant electron density within bonding distance of C(26) but also by the unfavorably short contact a fluorine atom at this site would make with a carbonyl oxygen atom [estimated F(26)···O(8) 2.5 Å]. In the refinement, due to shortage of data, the phenyl and cyclopentadienyl rings were constrained to idealized geometries (C−C 1.390 and 1.420 Å, respectively) and other chemically equivalent bond lengths within the molecule were constrained to be equal within an esd of 0.03 Å. The crystals of **5** and **24a** gave rather broad diffraction peaks and diffracted relatively poorly at high angles. In the case of **24a**, this may be attributed to the partial occupancy (50%) of a cavity within the crystal by a toluene solvent molecule disordered across an inversion center.

For **3** and **5**, refinement was based on *F*,[35] and for **4**, **9**, **17a**, and **24a**, refinement was based on *F²*.[36] The hydrogen atoms of the cyclopentadienyl rings were not included in structure factor calculations for **5** and **24a**, but those in **3**, **9**, and both molecules of **27a** were directly located and were included without refinement. All other hydrogen atoms were placed in calculated positions with displacement parameters fixed at a value of 0.10 Å² in **3** and **5** and set equal to 1.2 (methylene and phenyl) or 1.5*U*eq (methyl) of the parent carbon atoms for the other four structures. Semiempirical absorption corrections using ψ-scans were applied to the data of **3**, **5**, and **17a**,[36] and after initial refinement with isotropic displacement parameters, empirical absorption corrections were applied to the data of **4**, **9**, and **24a**.[37] Apart from the nitrogen and cyclopentadienyl carbon atoms in **9** (which tended to become nonpositive definite) and the carbon atoms of **5** (where there was a shortage of data), all full-occupancy non-hydrogen atoms were assigned anisotropic displacement parameters in the final cycles of full-matrix least-squares refinement.

Results and Discussion

Syntheses and Crystal Structures of the Heterodinuclear Complexes [MeSi{SiMe₂N(p-tol)}₃M−M′(CO)₂Cp] (M = Ti, Zr, Hf; M′ = Fe, Ru). The reactions of the complexes [MeSi-

(35) Sheldrick, G. M. SHELX 76: Program for Crystal Structure Determination. University of Cambridge, 1976.
(36) *SHELTXL*, PC version 5.03; Siemens Analytical Instruments Inc.: Madison, W1, 1994.
(37) Walker, N.; Stuart, D. *Acta Crystallogr., Sect. A.* **1983**, *39*, 158.

Table 1. Crystal Data and Refinement Parameters for Compounds **3**, **4**, **5**, **9**, **17a**, and **24a**

	3	**4**	**5**
empirical formula	$C_{35}H_{47}FeN_3O_2Si_4Ti$	$C_{35}H_{47}N_3O_2RuSi_4Ti$	$C_{35}H_{47}FeN_3O_2Si_4Zr$
fw	757.87	803.09	801.19
crystal system	monoclinic	monoclinic	monoclinic
space group	$P2_1/n$ (alt. No. 14)	$P2_1/n$ (alt. No. 14)	$P2_1/n$ (alt. No. 14)
a, Å	12.290(3)	12.424(3)	12.577(3)
b, Å	19.573(3)	19.497(4)	19.539(3)
c, Å	16.418(3)	16.504(4)	16.349(4)
β, deg	93.73(3)	93.63(2)	95.63(3)
V, Å³	3941.0(2)	3989.8(2)	3998.3(2)
Z	4	4	4
ρ_{calc}, Mg m⁻³	1.277	1.337	1.331
radiation (λ, Å)	Mo Kα (0.710 69)	Mo Kα (0.710 73)	Mo Kα (0.710 69)
μ, mm⁻¹	0.70	0.731	0.74
final R indices[a]			
$I > 2\sigma(I)$	$R = 0.0499$, $R' = 0.0479$[b]	$R_1 = 0.0431$, $wR_2 = 0.1042$	$R = 0.0543$, $R' = 0.0541$[b]
all data		$R_1 = 0.0744$, $wR_2 = 0.1418$	
weights: a, b[a]		0.0680, 0.8323	b
max and min $\Delta\rho$, e Å⁻³	0.394 and −0.394	1.042 and −0.934	0.521 and −0.417

	9	**17a**	**24a**·¹/₂tol
empirical formula	$C_{32}H_{38}FeN_3O_2Si_4Ti$	$C_{37}H_{50}N_4O_2RuSi_4Ti$	$C_{40.75}H_{55.75}N_3O_4RuSi_4Zr$
fw	769.76	844.14	1020.40
crystal system	monoclinic	monoclinic	triclinic
space group	$P2_1/c$ (No. 14)	$P2_1/c$ (No. 14)	$P\bar{1}$ (No. 2)
a, Å	19.903(2)	10.815(2)	12.426(3)
b, Å	10.572(4)	37.894(9)	14.510(3)
c, Å	19.111(3)	20.798(4)	16.742(4)
α, deg			115.406(17)
β, deg	112.939(9)	100.554(14)	96.302(13)
γ, deg			96.682(15)
V, Å³	3703.5(14)	8380(3)	2665.0(10)
Z	4	8	2
ρ_{calc}, Mg m⁻³	1.381	1.338	1.272
radiation (λ, Å)	Mo Kα (0.710 73)	Mo Kα (0.710 73)	Mo Kα (0.710 73)
μ, mm⁻¹	0.784	0.701	0.683
final R indices[a]			
$I > 2\sigma(I)$	$R_1 = 0.0974$, $wR_2 = 0.1248$	$R_1 = 0.0586$, $wR_2 = 0.1212$	$R_1 = 0.0705$, $wR_2 = 0.1505$
all data	$R_1 = 0.2591$, $wR_2 = 0.1574$	$R_1 = 0.1230$, $wR_2 = 0.1606$	$R_1 = 0.1602$, $wR_2 = 0.1758$
weights: a, b[a]	0.0384, 0.0000	0.0548, 19.6040	0.0833, 0.0000
max and min $\Delta\rho$, e Å⁻³	0.323 and −0.334	0.666 and −1.206	0.656 and −0.878

[a] $S = [\sum w(F_o^2 - F_c^2)^2/(n - p)]^{1/2}$ where n = number of reflections and p = total number of parameters; $R_1 = \sum||F_o| - |F_c||/\sum|F_o|$, $wR_2 = \sum[w(F_o^2 - F_c^2)^2]/\sum[w(F_o^2)^2]^{1/2}$, $w^{-1} = [\sigma^2(F_o)^2 + (aP)^2 + bP]$, $P = [\max(F_o^2, 0) + 2(F_c^2)]/3$. [b] For **3** and **5**, weights of $1/\sigma2(F)$ were applied [$I/\sigma(I) > 3$]; $R = \sum(\Delta F)/\sum(F_o)$; $R' = [\sum(\Delta F)^2/\sum w(F_o)^2]^{1/2}$.

Scheme 1. Synthesis of the Heterodinuclear Complexes **3−8**
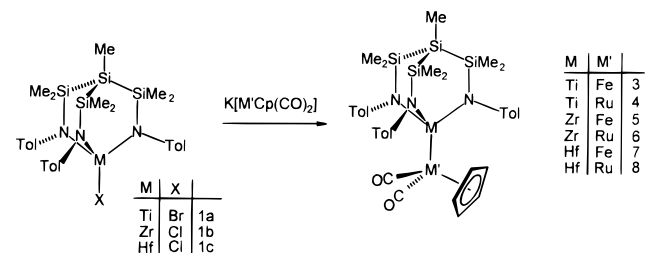
{SiMe₂N(*p*-tol)}₃MX] (M/X: Ti/Br, **1a**; Zr/Cl, **1b**; Hf/Cl, **1c**) with K[CpM′(CO)₂] afforded the metal−metal bonded complexes [MeSi{SiMe₂N(*p*-tol)}₃M−M′(CO)₂Cp] (**3−8**) (Scheme 1), all of which are thermally stable in the solid state and in solution. Although monitoring the reactions by ¹H NMR spectroscopy indicated almost quantitative conversions to the desired heterodinuclear compounds, the isolated yields were moderate (26−75%) due to losses upon crystallization from the reaction mixtures.

Since **3−8** contain identical sets of ligands, a meaningful comparison of the effect the metal−metal bonding has upon the electron density at the late transition metal center is possible by comparing the ν(CO) IR frequencies (Table 2). The effect

of replacing Ti by Zr (Hf) is evident in the comparison of **3** and **4** with **5** and **6** (**7** and **8**), the increased ionic character of the zirconium and hafnium complexes **5−8** being reflected in a shift of the ν(CO) bands (recorded in toluene) from 1978, 1931 cm⁻¹ in [Ti−Fe] **3** and 1991, 1937 cm⁻¹ in [Ti−Ru] **4** to 1961, 1910 cm⁻¹ in **5** (1969, 1915 cm⁻¹ in **7**) and 1986, 1932 cm⁻¹ in **6** (1987, 1933 cm⁻¹ in **8**). The reason for this trend may be related to the fact that, as previous theoretical studies of early−late heterobimetallics have shown, there may be significant π-donor−acceptor interaction apart from the dominating σ-bonding between the metals.[8,30] Within this line of reasoning, the Ti fragment is the better π-acceptor and thus allows a greater degree of charge redistribution from the late transition metal to the early transition metal.

It is interesting to compare the positions of the carbonyl bands in **3** and **4** with those found by Selegue and Sartain for [(Me₂N)₃-Ti−M′Cp(CO)₂][19] as well as those previously determined by us for related Ti−M′ heterodinuclear complexes (Table 2).[20] It is readily apparent that, in the systems containing the tripodal ligands, the ν(CO) bands are shifted to significantly higher wavenumbers, in comparison to those of the [M′Cp(CO)₂]⁻ anions than they are for Selegue's complexes stabilized by monodentate amido ligands. This implies that there is a greater charge redistribution between the nucleophilic {MCp(CO)₂} and

Table 2. Infrared Carbonyl Stretching Frequencies of the M—M′ Heterodinuclear Complexes Reported in this Work as Well as in Previous Studies

complex	$\nu(CO)$ (ν_s, ν_{as}), cm^{-1}	ref
Ti—Fe		
[(Me₂N)₃Ti—Fe(CO)₂Cp]	1948, 1898	20
[MeSi{SiMe₂N(p-tol)}₃Ti—Fe(CO)₂Cp] (**3**)	1978, 1931	this work
[MeSi{SiMe₂N(2-FC₆H₄)}₃Ti—Fe(CO)₂Cp] (**9**)	1980, 1932	this work
Ti—Ru		
[(Me₂N)₃Ti—Ru(CO)₂Cp]	1972, 1911	19
[MeSi{SiMe₂N(p-Tol)}₃Ti—Ru(CO)₂Cp] (**4**)	1991, 1937	this work
[MeSi{SiMe₂N(2-FC₆H₄)}₃Ti—Ru(CO)₂Cp] (**10**)	1997, 1940	this work
Zr—Fe		
[Cp₂(Me)Zr—Fe(CO)₂Cp]	1937, 1872	14
[CH₂(CH₂NSiMe₃)₂(Cp)Zr—Fe(CO)₂Cp]	1947, 1895	38
[MeSi{SiMe₂N(p-tol)}₃Zr—Fe(CO)₂Cp] (**5**)	1961, 1910	this work
[MeSi{SiMe₂N(2-FC₆H₄)}₃Zr—Fe(CO)₂Cp] (**11**)	1968, 1914	this work
Zr—Ru		
[Cp₂(Me)Zr—Ru(CO)₂Cp]	1950, 1880	14
[CH₂(CH₂NSiMe₃)₂(Cp)Zr—Ru(CO)₂Cp]	1957, 1895	38
[MeSi{SiMe₂N(p-tol)}₃Zr—Ru(CO)₂Cp] (**6**)	1986, 1932	this work
MeSi{SiMe₂N(2-FC₆H₄)}₃Zr—Cu(CO)₂Cp (**12**)	1974, 1929	this work
Hf—Fe		
[MeSi{SiMe₂N(p-tol)}₃Hf—Fe(CO)₂Cp] (**7**)	1969, 1915	this work
MeSi{SiMe₂N(2-FC₆H₄)}₃Hf—Fe(CO)₂Cp (**13**)	1971, 1917	this work
Hf—Ru		
[MeSi{SiMe₂N(p-tol)}₃Hf—Ru(CO)₂Cp] (**8**)	1987, 1933	this work
[MeSi{SiMe₂N(2-FC₆H₄)}₃Hf—Ru(CO)₂Cp] (**14**)	1979, 1934	this work

the Lewis acidic Ti complex fragment in the systems stabilized by the amido tripod. This trend may be related to structural characteristics of the compounds in question which are discussed below. There is an equally striking difference in the carbonyl band positions between those of compounds **5** and **6** and of the previously characterized complexes [CH₂(CH₂NSiMe₃)₂(Cp)-Zr—M′Cp(CO)₂][38] as well as those of [Cp₂(X)Zr—M′Cp-(CO)₂][14−18] (Table 2). Apparently, less electron density is withdrawn from the carbonylmetal fragment by the 16-electron fragment [Cp₂ZrX]⁺ than by the 14-electron fragment [Cp-(amide)₂Zr]⁺. The Lewis acidity at Zr is in turn markedly further increased on going to the 12-electron fragment [(tripodtriamide)-Zr]⁺.

To confirm the proposed structural arrangement in **3—8**, single-crystal X-ray structure analyses of **3—5** were carried out. The molecular structures of all three compounds in the crystal are virtually identical, and two different views of **3** and **5** are provided in Figure 1 and the principal bond lengths and interbond angles of all three complexes are listed in Table 3.

The ligand framework and the peripheral tolyl groups of the amido ligand shield the coordination sphere of the tetravalent zirconium, which is part of a molecular cage thus formed, leaving a cone-shaped "binding site" which accommodates the iron complex fragment. The dimensions of the "cone"-like environment surrounding the binding site appear to be "fine-tuned" to the requirement of the second complex fragment by slight rotations of the phenyl rings about the Ph—N vector. In an idealized C_{3v} structure, maximum cone volume would occur when all three aryl groups radiate out with a torsion angle of 90° about the N—C(aryl) vector, relative to the Si—N bond [mean of C(n2)—C(n1)—N(n)—Si(n) and C(n6)—C(n1)—N(n)—Si(n), n = 1—3]. In each of the three complexes **3—5**, one tolyl ring [C(11)—C(16)] is approximately in this idealized conforma-

(38) Friedrich, S.; Gade, L. H.; Scowen, I. J.; McPartlin, M. *Organometallics* **1995**, *14*, 5344.
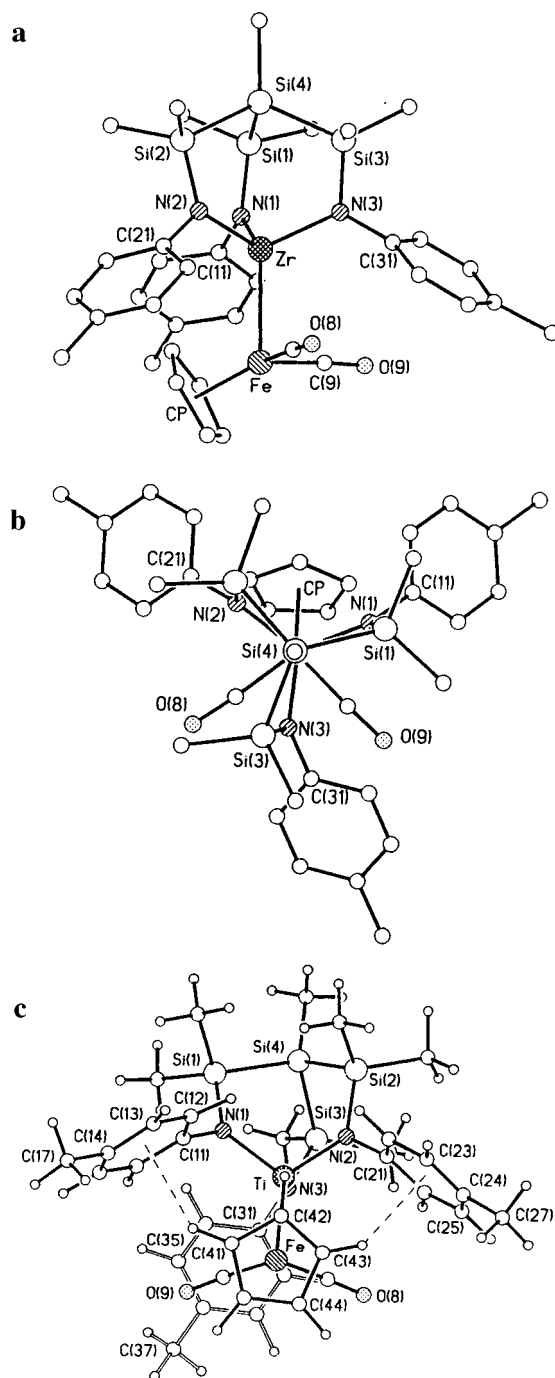
Figure 1. Isostructural molecules present in the crystals of **3—5**: (a) MeSi{SiMe₂N(p-tol)}₃Zr—Fe(CO)₂Cp] (**5**) viewed perpendicular to the metal—metal bond, showing the lampshade arrangement of the tolyl groups; (b) [MeSi{SiMe₂N(p-tol)}₃Ti—Ru(CO)₂Cp] (**4**) viewed along the Ti—Ru axis, showing the staggered conformation of the halves of the molecule; (c) [MeSi{SiMe₂N(p-tol)}₃Ti—Fe(CO)₂Cp] (**3**) viewed perpendicular the Cp ring to show the H···π-arene interactions with two tolyl rings [H(43)···centroid 2.45 and H(41)···centroid 2.50 Å]. Principal interatomic distances and angles are listed in Table 3.

tion with deviations of mean torsion angles from orthogonality of 1.0° in **3**, 2.2° in **4**, and 2.9° in **5**. The other two tolyl rings in each structure are rotated from the orthogonal conformation, toward each other, apparently to optimize π-arene···H interactions with the Cp ring of the M′(CO)₂Cp fragment as shown in Figure 1c for the Ti—Fe compound (**3**); the [C(31)—C(36)] ring is rotated 2.8° in **3**, 4.5° in **4**, and 7.9° in **5** and the [C(21)—C(26)] ring shows the very large deviations from orthogonality of 23.5° in **3**, 18.7° in **4**, and 17.5° in **5**.

Table 3. Selected Interatomic Distances and Angles for **3**, **4**, **5**, **9**, **17a**, and **24a**

	3 M = Ti M′ = Fe	**4** M = Ti M′ = Ru	**5** M = Zr M′ = Fe	**9** M = Ti M′ = Fe	**17a** mol. 1	mol. 2	**24a** M = Zr M′ = Ru
			(a) Distances (Å)				
M−M′	2.460(1)	2.5609(8)	2.605(2)	2.433(4)			
M−N(1)	1.934(4)	1.941(3)	2.080(9)	1.935(9)	1.978(5)	1.972(5)	2.100(8)
M−N(2)	1.941(4)	1.947(3)	2.088(9)	1.935(8)	1.996(5)	1.987(5)	2.120(7)
M−N(3)	1.930(4)	1.927(3)	2.065(9)	1.941(9)	1.934(5)	1.936(5)	2.120(7)
M−N(4)					2.006(5)	2.001(5)	
M−C(41)					2.067(6)	2.061(7)	
M′−Cp[a]	1.732(5)	1.933(4)	1.725(11)	1.726(8)	1.912(7)	1.915(7)	1.919(11)
M′−C(8)	1.735(6)	1.863(5)	1.757(13)	1.689(12)	1.858(8)	1.871(8)	2.083(9)
M′−C(9)	1.745(6)	1.876(4)	1.741(15)	1.681(12)	1.875(9)	1.866(9)	1.881(13)
M′−C(41)					2.033(6)	2.020(7)	
Si(1)−Si(4)	2.348(2)	2.350(2)	2.354(5)	2.324(6)	2.326(3)	2.336(3)	2.336(4)
Si(2)−Si(4)	2.326(2)	2.329(2)	2.340(6)	2.322(6)	2.335(3)	2.328(3)	2.339(5)
Si(3)−Si(4)	2.335(2)	2.339(2)	2.326(6)	2.333(6)	2.333(3)	2.323(3)	2.361(4)
Si(1)−N(1)	1.764(4)	1.762(3)	1.747(10)	1.770(10)	1.744(6)	1.734(5)	1.758(7)
Si(2)−N(2)	1.766(5)	1.764(3)	1.720(10)	1.761(9)	1.755(5)	1.738(5)	1.759(8)
Si(3)−N(3)	1.753(4)	1.763(3)	1.736(10)	1.759(9)	1.749(3)	1.743(6)	1.749(7)
N(1)−C(11)	1.446(6)	1.437(5)	1.417(15)	1.412(12)	1.414(8)	1.419(8)	1.440(11)
N(2)−C(21)	1.441(7)	1.441(5)	1.458(15)	1.450(12)	1.395(6)	1.394(8)	1.437(12)
N(3)−C(31)	1.439(7)	1.440(5)	1.436(16)	1.447(10)	1.425(8)	1.436(8)	1.427(12)
N(4)−C(41)					1.267(7)	1.260(8)	
Si(1)···Si(2)	3.637(3)	3.635(3)	3.717(7)	3.649(7)	3.638(4)	3.639(4)	3.670(5)
Si(1)···Si(3)	3.743(3)	3.750(3)	3.761(7)	3.661(7)	3.710(4)	3.684(4)	3.701(5)
Si(2)···Si(3)	3.603(3)	3.612(3)	3.704(7)	3.623(7)	3.682(4)	3.730(4)	3.741(5)
N(1)···N(2)	3.119(6)	3.124(6)	3.308(12)	3.119(10)	3.161(7)	3.124(7)	3.220(10)
N(1)···N(3)	3.064(6)	3.075(6)	3.276(12)	3.133(10)	3.240(7)	3.229(7)	3.274(10)
N(2)···N(3)	3.116(6)	3.139(6)	3.332(12)	3.048(10)	3.211(7)	3.258(7)	3.364(10)
			(b) Angles (deg)				
N(1)−M−M′/CN[a]	113.9(1)	113.8(1)	114.9(3)	110.5(3)	110.1(2)	111.0(2)	
N(2)−M−M′/CN[a]	111.8(1)	110.4(1)	112.5(3)	112.4(3)	114.2(2)	110.7(2)	
N(3)−M−M′/CN[a]	111.4(1)	111.7(1)	112.6(3)	114.4(3)	105.9(2)	107.3(2)	
N(1)−M−N(2)	107.2(2)	107.0(1)	107.4(4)	105.4(2)	104.2(2)	99.3(3)	
N(1)−M−N(3)	104.9(2)	105.3(1)	104.4(4)	107.9(5)	111.8(2)	111.4(2)	101.7(3)
N(2)−M−N(3)	107.2(2)	108.3(1)	106.7(4)	103.7(4)	109.6(2)	112.3(2)	105.0(3)
Si(1)−Si(4)−Si(2)	102.2(10)	101.98(7)	104.7(2)	103.5(2)	102.6(1)	102.6(1)	103.4(2)
Si(1)−Si(4)−Si(3)	106.1(1)	106.22(6)	106.9(2)	103.6(2)	105.6(1)	104.5(1)	104.0(2)
Si(2)−Si(4)−Si(3)	101.2(1)	101.39(6)	105.1(2)	102.2(2)	104.2(1)	106.6(1)	105.5(2)
Si(4)−Si(1)−N(1)	103.8(2)	104.0(1)	104.6(4)	103.7(4)	104.7(2)	104.5(2)	104.2(3)
Si(4)−Si(2)−N(2)	102.0(2)	102.9(1)	102.9(4)	100.8(4)	102.9(2)	102.4(2)	102.8(3)
Si(4)−Si(3)−N(3)	103.0(2)	102.7(1)	104.4(4)	103.5(4)	101.6(2)	101.1(2)	103.7(3)
M−N(1)−Si(1)	121.2(2)	120.8(2)	119.5(5)	118.9(6)	115.1(3)	115.1(3)	120.4(4)
M−(N2)−Si(2)	122.4(2)	121.5(2)	121.9(5)	121.6(6)	115.1(3)	115.1(3)	120.1(4)
M−N(3)−Si(2)	119.4(2)	119.5(2)	118.9(5)	119.1(5)	118.3(3)	118.2(3)	120.9(4)
M−N(1)−C(11)	123.3(3)	122.6(2)	122.4(8)	124.1(7)	129.9(4)	129.0(4)	112.2(6)
M−N(2)−C(21)	124.2(3)	124.4(3)	121.4(7)	120.5(6)	123.4(4)	121.3(4)	120.7(6)
M−N(3)−C(31)	123.5(3)	123.0(2)	121.3(7)	127.0(6)	124.2(4)	123.6(4)	116.1(6)
Si(1)−N(1)−C(11)	115.3(3)	116.3(2)	118.0(8)	117.0(7)	114.5(4)	115.8(4)	112.2(6)
Si(2)−N(2)−C(21)	113.2(3)	113.8(2)	116.3(8)	117.0(6)	121.2(4)	121.3(4)	118.3(6)
Si(3)−N(3)−C(31)	115.8(3)	111.7(6)	118.6(7)	113.7(7)	116.9(4)	117.0(4)	116.1(6)
Cp[a]−M′−M/C(41)	121.7(2)	120.7(2)	117.3(5)	121.7(3)	119.4(3)	119.6(3)	
M−M′−C(8)	83.9(2)	82.8(1)	83.9(5)	85.4(6)			
M−M′−C(9)	88.1(2)	87.7(1)	88.9(5)	88.7(5)			
C(8)−M′−Cp[a]	127.1(2)	128.8(2)	128.9(5)	126.4(6)	127.8(3)	126.5(3)	123.4(5)
C(9)−M′−Cp[a]	126.1(2)	127.9(2)	127.4(5)	127.7(6)	125.6(3)	126.7(3)	129.0(5)
C(8)−M′−C(9)	97.3(3)	94.6(2)	96.6(6)	94.6(7)	91.9(4)	92.7(4)	87.8(4)

[a] Midpoint of relevant atoms used for the Cp ring and for N(4)−C(41).

The orientation of the carbonyl ligands at the iron center is such that their interpretation as potentially semibridging may be ruled out [∠{C(8)−Fe−M}: 83.9(2)° (**3**), 82.8(1)° (**4**), 83.9(5)° (**5**). ∠{C(9)−Fe−M}: 88.1(2)° (**3**), 87.7(1)° (**4**), 88.9(5)° (**5**). d{C(8)−M}: 2.856 Å (**3**), 2.972 Å (**4**), 2.983 Å (**5**). d{C(9)−M}: 2.968 Å (**3**), 3.113 Å (**4**), 3.105 Å (**5**)], and the metal−metal bond is therefore truly unsupported. The relatively short metal−metal distances of 2.460(1) Å (Ti−Fe in **3**), 2.5609(8) Å (Ti−Ru in **4**), and d(Zr−Fe) = 2.605(2) Å in the crystal structures of the complexes indicate that there is little significant repulsive interaction between the two complex fragments joined by the Fe−Zr and Ti−Fe bonds. On the other hand, due to the steric demand of the ligands at both metal

centers which adopt a staggered arrangement in the crystal structures, the internal rotation about the metal−metal vector is hindered in the case of the Ti−M complexes. For the Ti−Fe compound, the high-temperature limit is observed at temperatures above 330 K (spectral patterns indicating 3-fold symmetry of the Ti-complex fragment). The rotation around the Ti−Fe axis may, however, be frozen out on the NMR time scale upon cooling to 245 K; the effective symmetry of the molecule is thus reduced to C_s. The free activation enthalpy of this process was determined to be $\Delta G^{\ddagger} = 57$ kJ mol^{-1}.

Syntheses and Characterizations of the Heterodinuclear Complexes [MeSi{SiMe₂N(2-FC₆H₄)}₃M−M′(CO)₂Cp] (M = Ti, Zr, Hf; M′ = Fe, Ru). We previously reported the synthesis
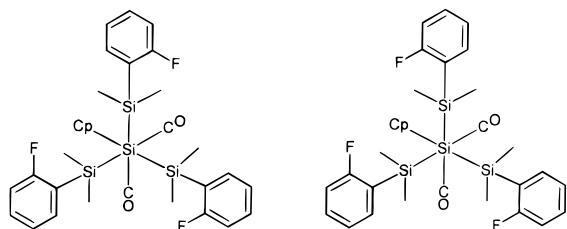
Figure 2. The two conformers of the complexes **9** and **10** defined by the orientation of the 2-fluorophenyl groups.

Scheme 2. Synthesis of the Heterodinuclear Complexes **9**–**14**
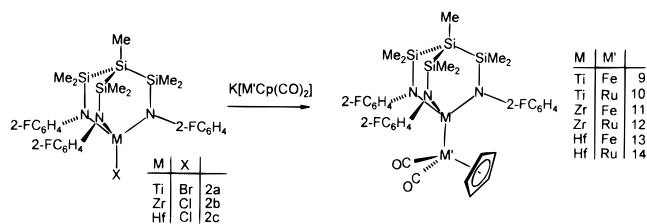
of tripodal amido ligands of the type employed in this study in which the peripheral tolyl groups are replaced by 2-FC$_6$H$_4$ groups which potentially enable additional weak coordination to the Lewis acidic early transition metal center through the ortho fluorine atoms.[28,39] The increased shielding of the metal leads to greater stability of the complexes which may be handled under somewhat less rigorous conditions of exclusion of air and moisture. Reaction of the complexes [MeSi{SiMe$_2$N(2-FC$_6$H$_4$)}$_3$-MX] (M/X: Ti/Br, **2a**; Zr/Cl, **2b**; Hf/Cl, **2c**) with K[M′Cp-(CO)$_2$] yielded the corresponding heterodinuclear complexes [MeSi{SiMe$_2$N(2-FC$_6$H$_4$)}$_3$M–M′(CO)$_2$Cp] (**9**–**14**) (Scheme 2).

The spectroscopic properties of the zirconium and hafnium derivatives are very similar to those of **5**–**8**. For the Ti–Fe and Ti–Ru complexes, however, complicated signal patterns in the ^{1}H and ^{13}C NMR spectra at ambient temperature indicated that the rapid motion of the peripheral aryl groups as well as the internal rotation around the metal–metal bond axis is slow on the NMR time scale. Although the complicated nature of the ^{1}H NMR spectra of **10** recorded within a temperature range of 213 and 353 K (in toluene-d_8) did not permit a complete analysis of the dynamic processes involved, we interpret the fact that two sharp signals are observed for the Cp–H nuclei at 213 K as indicating the presence of two conformers which arise due to a different orientation of the *o*-fluorophenyl groups (Figure 2).

Both conformers of **10** give rise to resonances of approximately equal intensities [δ(Cp) = 3.92 and 4.14 in toluene-d_8]. Coalescence of these two singlet resonances is observed at T_c = 342 K (200.13 MHz), and an activation enthalpy for the interconversion of the conformers of $\Delta G^{\ddagger}$ = 72 kJ mol^{-1} may be estimated from these data. A similar situation was found for the Ti–Fe analogue **9**; however, coalescence of the two Cp signals [δ(Cp) = 3.45 and 3.63] was not observed below 350 K, at which point rapid decomposition of the complex in solution set in.

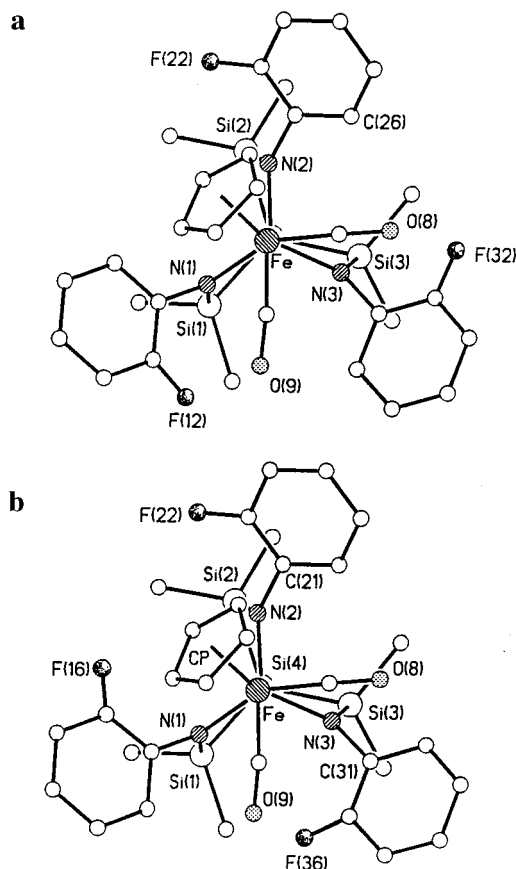The presence of two conformers due to different orientations of the peripheral *o*-fluorophenyl groups is also reflected in the disorder between the different fluorine positions in the crystal structure of compound **9**. This disorder, attributable to a random

(39) Memmler, H.; Walsh, K.; Gade, L. H.; Lauher, J. W. *Inorg. Chem.* **1995**, *34*, 4062.

Figure 3. Structures of the two conformers of [MeSi{SiMe$_2$N(2-FC$_6$H$_4$)}$_3$Ti–Fe(CO)$_2$Cp] (**9**) shown by X-ray structure determination to be randomly disordered in a 60:40 ratio in the solid state: (a) the 60% conformer; (b) the 40% conformer. Each of the fluorine atoms is involved in a short F···H(Me) contact consistent with some hydrogen-bonding interaction [mean F···H(Me) 2.36 Å]. The overall structure and numbering are similar to those shown in Figure 1a for **5**, and principal interatomic distances and angles are listed in Table 2.

distribution of the two conformers throughout the crystal in 60% (**A**) and 40% (**B**) ratio, may explain the poor diffraction by this crystal. Despite the shortage of data and the relatively high esd's on all metric parameters, the overall structures of the two conformers are established unambiguously and are illustrated in Figure 3; the principal bond lengths and angles are listed with those of the other complexes in Table 3.

The metal complex fragment {FeCp(CO)$_2$} represents a bulky "ligand" at the titanium center and therefore blocks the coordination of the fluorine groups and enforces the "lamp shade" arrangement of the peripheral aryl groups. The Ti–Fe bond length of 2.433(4) Å, which lies at the lower end for such metal–metal bonds,[19,29,30] indicates that there is relatively little mutual repulsion between the ligand spheres of the two metal centers. This may be seen as an additional indication in favor of the interpretation of the dynamic NMR spectra in terms of the hindered rotation of the fluorophenyl groups.

Comparison of the Molecular Structures of the Metal–Metal Bonded Heterodinuclear Complexes. Comparison of the data for the four metal–metal bonded complexes gives some insight into the way the tripodal ligands adapt to the requirements of the Group 4 metal and how the cone-shaped "binding site" adjusts to accommodate the second complex fragment (Table 4). The change from Ti to Zr in these compounds is accompanied by a significant increase in the N···N donor distances presented by the tridentate ligand, which increase from a mean of 3.104 Å for the Ti compounds (**3**, **4**, and **9**) to a

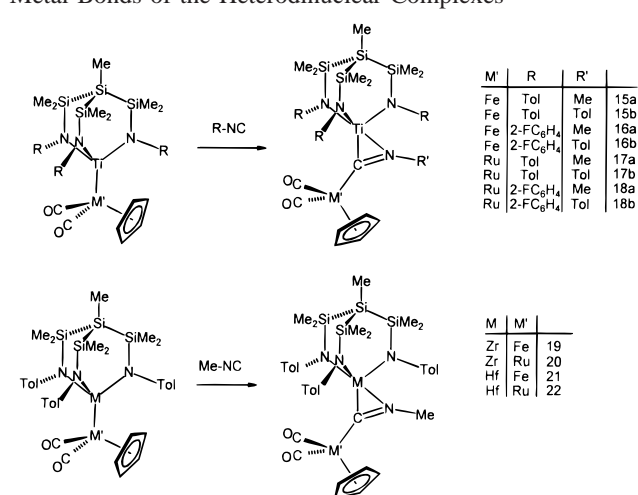**Table 4.** Selected Mean Angles and Interatomic Distances for **3**, **4**, **5**, **9**, **17a**, and **24a**

	3	**4**	**5**	**9**	**17a** mol. 1	**17a** mol. 2	**24a**
			Angles (deg)				
Si−Si−N	102.9	103.2	104.0	102.7	103.1	102.7	103.6
Si−N−Ph	114.8	113.9	117.6	115.9	117.5	118.0	115.5
M−N−Ph	123.7	123.3	121.7	123.9	125.8	124.6	116.3
M−N−Si	121.0	120.6	120.1	119.9	116.2	116.1	120.5
N−M−N	106.4	106.9	105.4	106.3	108.9	109.3	102.0
			Interatomic Distances (Å)				
N···N (amido)	3.100	3.113	3.305	3.100	3.204	3.204	3.286
M−N	1.935	1.938	2.078	1.937	1.969	1.965	2.133
Si−Si	2.336	2.339	2.339	2.326	2.331	2.329	2.345

mean of 3.305 Å for the Zr complex (**4**). This flexibility of the ligand means that, despite the greater Zr−N bond lengths (mean 2.078 Å) compared to the Ti−N distances (mean 1.937 Å), there is a relatively small decrease in the angles subtended by the ligand at the metal in going from Ti (mean N−Ti−N angle 106.5°) to Zr (mean N−Zr−N angle 105.4°). The Si−Si and Si−N bond lengths in the four compounds do not differ significantly from their mean values of 2.335 and 1.755 Å, respectively, and it appears that the flexibility shown by the ligand derives from significant enlargement of all the angles at Si in going from Ti to Zr. The mean Si−Si−Si angle at Si(4) increases from 103.2° in the Ti compounds (**3**, **4**, and **9**) to 105.6° in the Zr compound (**5**), and similarily the mean Si−Si−N angle increases from 102.9 to 104.0°.

In the crystal structure of compound **9**, the fluorophenyl rings adopt an approximately propeller-like conformation with fairly large deviations (range 10.6−27.0°) from the orthogonal orientation, an arrangement that appears to be dictated by the steric requirements of the ortho fluorine substituents. Unlike the tolyl compounds **3**−**5**, the greater restriction on rotation of the fluorophenyl rings in **9** results in only one cyclopentadienyl H-bonding interaction with a C(21)−C(26) ring [arene centroid to H(45) distance 2.445 Å].

Insertion of Isonitriles into the Polar Metal−Metal Bonds of the Heterodinuclear Complexes. Preliminary studies of the reactivity of the early−late heterodinuclear complexes reported in this study revealed a reactive behavior toward polar unsaturated organic substrates which may be rationalized in terms of a cooperative interaction of a transition metal nucleophile and an electrophile.[32,33] This type of reactivity is reflected in the insertion of isonitriles into the polar metal−metal bond to give dinuclear metallaiminoacyl complexes as is shown in Scheme 3.

Upon reaction of compounds **3**−**10** with 1 molar equiv of an isocyanide, immediate insertion into the polar metal−metal bond takes place, generating [MeSi{SiMe$_2$N(R)}$_3$Ti{η^2-(C=NR′)M′(CO)$_2$Cp}] (R = *p*-tol, 2-FC$_6$H$_4$; R′ = Me, *p*-tol; M′ = Fe, Ru (**15a,b**−**18a,b**)) as well as [MeSi{SiMe$_2$N(*p*-tol)}$_3$M{η^2-(C=NMe)M′(CO)$_2$Cp}] (M = Zr, Hf) (Scheme 3). This may be viewed as a true metal analogue of the well-established α-addition reaction of an electrophile and a nucleophile to the carbon atom in isocyanide chemistry,[40] a type of reactivity also observed in reactions of early transition metal alkyl or silyl compounds with isocyanides.[41,42] The only previous example of such an insertion into a (halide-supported) formal

(40) Saegusa, T.; Ito, Y. In *Organic Chemistry*; Ugi, I., Ed.; Academic Press: New York, 1971; Vol. 20.
(41) Lappert, M. F.; Luong-Thi, N. T.; Milne, C. R. C. *J. Organomet. Chem.* **1979**, *174*, C35.
(42) Durfee, L. D.; Rothwell, I. P. *Chem. Rev.* **1988**, *88*, 1061.

Scheme 3. Insertion of Isonitriles into the Polar Metal−Metal Bonds of the Heterodinuclear Complexes

M′	R	R′	
Fe	Tol	Me	15a
Fe	Tol	Tol	15b
Fe	2-FC$_6$H$_4$	Me	16a
Fe	2-FC$_6$H$_4$	Tol	16b
Ru	Tol	Me	17a
Ru	Tol	Tol	17b
Ru	2-FC$_6$H$_4$	Me	18a
Ru	2-FC$_6$H$_4$	Tol	18b

M	M′	
Zr	Fe	19
Zr	Ru	20
Hf	Fe	21
Hf	Ru	22

Table 5. ^{13}C NMR Chemical Shifts Assigned to the Carbon Nuclei of the Metallaminoacyl Groups in [MeSi{SiMe$_2$N(*p*-tol)}$_3$M-{η^2-C(=NMe)M′Cp(CO)$_2$}] (Recorded in C$_6$D$_6$)

complex	M, M′	δ{M^{13}C-(=NMe)M′}	complex	M, M′	δ{M^{13}C-(=NMe)M′}
15a	Ti, Fe	277.3	**20**	Zr, Ru	278.4
17a	Ti, Ru	267.3	**21**	Hf, Fe	303.8
19	Zr, Fe	289.3	**22**	Hf, Ru	292.4

metal−metal bond between transition metals has been the reaction of the fulvalene-bridged complex (C$_{10}$H$_8$)Cp$_2$Zr$_2$Cl$_2$ with Bu^t−NC reported by Herrmann et al.,[43] which, in view of the lack of M−M bond polarity in that system, cannot be related to the α-addition pattern.

The unusual environment of the bridging carbon atom of the metallaiminoacyl fragment gives rise to remarkably low field chemical shifts of the corresponding signals in the ^{13}C NMR spectra. The way in which the different combinations of metals influence this characteristic spectroscopic probe for the insertion products is particularly apparent upon comparison of the data obtained for the closely related compounds [MeSi{SiMe$_2$N(*p*-tol)}$_3$Ti{η^2-(C=NMe)M′(CO)$_2$Cp}] (**15a**, **17a**, and **19**−**22**), which are summarized in Table 5.

On going from Ru to Fe and from Ti to Hf, the signals of the MC(NR)M′ ^{13}C nuclei are shifted considerably to lower field, the extremes being represented by the Ti−Ru and the Fe−Hf complexes [δ(^{13}C) 267.8 and 303.8, respectively]. This reflects the differences in donor and acceptor properties of the metal complex fragment, although a more detailed analysis would require a systematic theoretical study of this effect.

To unambiguously establish the structure of the insertion products, a single-crystal X-ray structure analysis of compound **17a** was carried out. There are two independent molecules in the crystal of virtually identical geometries, the only significant difference being in a slight change in the conformations of the tolyl rings. The structure of the first molecule is illustrated in Figure 4, and the principal metric parameters for the two molecules are listed in Table 3.

The result of the crystal structure analysis cleary establishes the nature of the insertion products as formulated on the basis of the spectroscopic data. The metallaiminoacyl fragment is coordinated to the Ti center in a fashion very similar to that found previously for ordinary (iminoacyl)titanium complexes

(43) Herrmann, W. A.; Cuenca, T.; Menjon, B.; Herdtweck, E. *Angew. Chem., Int. Ed. Engl.* **1987**, *26*, 697.

a

b
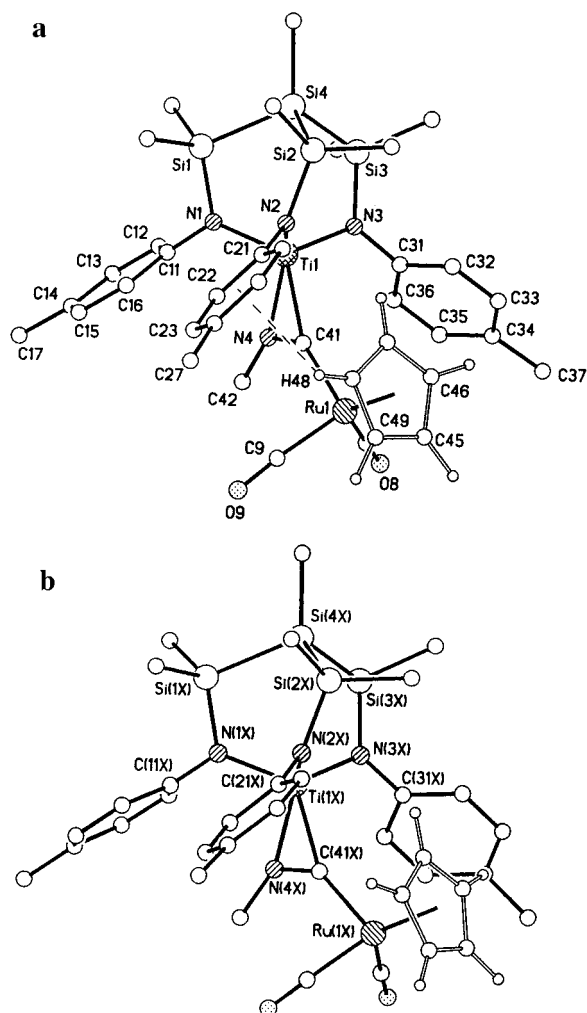
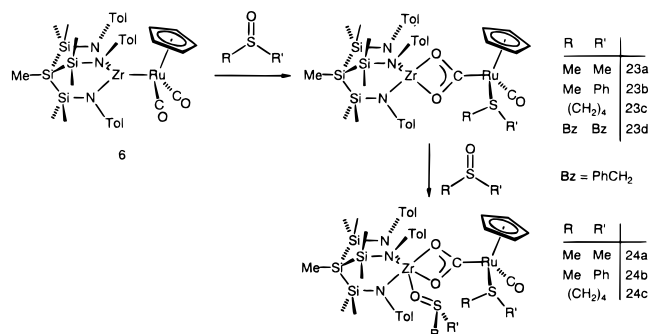**Figure 4.** Molecular structures of the two independent molecules of [MeSi{SiMe$_2$N(*p*-tol)}$_3$Ti(η^2-C=NMe)}$_3$Ru(CO)$_2$Cp] (**17a**): (a) the first molecule showing the numbering scheme and the close contact between the Cp ring and the second tolyl group; (b) the second molecule which differs from the first only in orientation of the tolyl rings [this can most readily be seen here for ring C(11X)]. Principal interatomic distances and angles for both molecules are listed in Table 2 for comparison with **4**.

derived from the insertion of isonitriles into Ti–C bonds. The mean bond lengths in **17a** of Ti–C(41) 2.064(6), Ti–N(4) 2.004(5), and C(41)–N(4) 1.264 Å are similar to the respective equivalent lengths of 2.080(6), 2.125(5), and 1.240(6) Å in [Cp$_2$Ti{η^2-CN^{t}Bu(Me)(CN^{t}Bu)}](BPh$_4$)[44] and those of 2.086(6), 2.025(5), and 1.279 Å in [Ti(OC$_6$H$_3$-2,6-Ph$_2$){CNCH$_2$SiMe$_3$(CH$_2$-SiMe$_3$)}][45] and to those in other related systems.[46,47] Assuming that the iminoacyl fragment occupies one coordination site at the titanium atom [(N(4)–Ti–C(41) 36.2(2)°], this may be described as a distorted tetrahedral geometry.

The mean Ti–N distance in **17a** of 1.967(5) Å is significantly longer than that of 1.938(3) Å in its precursor **4**, and the mean N–Ti–N angle of 109.1(2)° in **17a** is also larger than of 106.9(1)° in **4**. The increase in these parameters on formation of the insertion product is accompanied by a marked increase

(44) Bochmann, M.; Wilson, L. M. *Organometallics* **1987**, *6*, 2556.
(45) Chamberlain, L. R.; Durfee, L. D.; Fanwick, P. E.; Kobriger, L.; Latesky, S. L.; McMullen, A. K.; Rothwell, I. P.; Folting, K.; Huffman, J. C.; Streib, W. E.; Wang, R. *J. Am. Chem. Soc.* **1987**, *109*, 390.
(46) Lubben, T. V.; Plössl, K.; Norton, J. R.; Miller, M. M.; Anderson, O. P. *Organometallics* **1992**, *11*, 122.
(47) Guram, A. S.; Jordan, R. F. *J. Org. Chem.* **1993**, *58*, 5595.

Scheme 4. Reaction of the Zr–Ru Complex **6** with Sulfoxides[a]

[a] Oxygen transfer from the sulfoxide to a carbonyl ligand to give CO$_2$-linked dinuclear complexes.
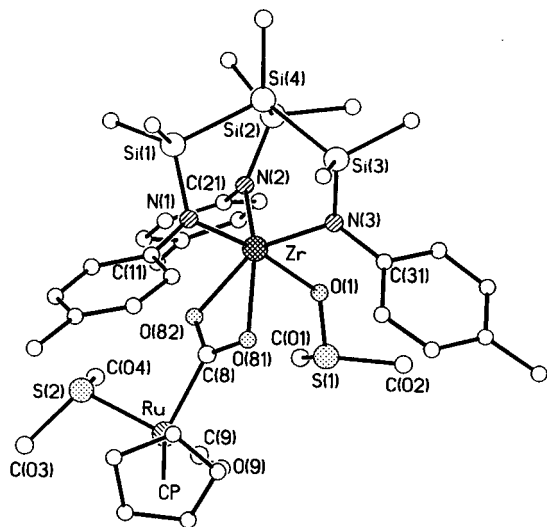
in the mean N···N donor atom distance from 3.113 in **4** to 3.204 Å in **17a** made possible by a corresponding increase in the mean Si–Si–Si angle from 103.2 to 104.4°.

In the adjustment to the steric requirements of the inserted ligand, a very asymmetrical arrangement of the tolyl groups has arisen. In the first independent molecule, the tolyl groups C(11) and C(31) are rotated from an orthogonal arrangement by 8.3 and 14.1°, respectively, in opposite directions, whereas in the second molecule, the corresponding rings rotate by 9.2 and 4.5° in the same directions, resulting in a dihedral angle between these pairs of rings of 59.3° in the first molecule and 68.4° in the second. The second ring [C(21)] in each molecule has an extremely high deviation from the orthogonal orientation (56.5 and 53.6°, respectively); in the first molecule, this results in a relatively close contact of 2.70 Å between the ring centroid and H(48) of the Cp ring, rather similar to the type observed in **3** (vide supra); all other contacts distances in both molecules correspond to normal van der Waals interactions.

Reaction of the Heterodinuclear Complex [MeSi-(SiMe$_2$NTol)$_3$Zr–RuCp(CO)$_2$] (6) with Sulfoxides. Upon reaction of 1 molar equiv amounts of Me$_2$SO, Ph(Me)SO, (CH$_2$)$_4$SO, and (PhCH$_2$)$_2$SO with the Zr–Ru heterodinuclear complex [MeSi(SiMe$_2$NTol)$_3$Zr–RuCp(CO)$_2$] (**6**) at −40 °C in toluene, immediate transformations occurred, yielding products which could be isolated as yellow solids by evaporation of the solvent in vacuo. On the basis of their analytical and ^{1}H and ^{13}C NMR as well as infrared spectroscopic properties, these were formulated as [MeSi{SiMe$_2$N(*p*-tol)}$_3$Zr(μ-O$_2$C)RuCp(CO)-{S(R)R'}] (R = R' = Me (**23a**); R = Me, R' = Ph (**23b**); R, R' = (CH$_2$)$_4$ (**23c**); R, R' = PhCH$_2$ (**23d**)) (Scheme 4). Products of higher crystallinity were obtained upon addition of a second equivalent of sulfoxide, giving μ-CO$_2$-linked dinuclear compounds containing an O-bonded sulfoxide ligand at the zirconium center but having otherwise compositional and spectroscopic properties analogous to those of [MeSi{SiMe$_2$N(*p*-tol)}$_3$Zr{OS(R)R'-κO}(μ-O$_2$C)RuCp(CO){S(R)R'}] (R = R' = Me (**24a**); R = Me, R' = Ph (**24b**); R, R' = (CH$_2$)$_4$ (**24c**)). No adduct formation was observed upon treating **23d** with a second equivalent of (PhCH$_2$)$_2$SO.

To establish the structure of the reaction products unambiguously, a single-crystal X-ray structure analysis of **24a** was carried out. The center piece of the molecular structure displayed in Figure 5 is the Zr($\mu_2\kappa^3$-O$_2$C)Ru unit in which the CO$_2$ formed in the reaction links the two metal centers. The geometrical characteristics of the carboxylato bridge [*d*{C(8)–O(81)} 1.276(11) Å, *d*{C(8)–O(82)} 1.297(11) Å, *d*{Ru–C(8)} 2.083(9) Å,, ∠{O(81)–C(8)–O(82)} 115.9(8)°] are similar to those found in a previously characterized CO$_2$-linked Zr–Ru heterodinuclear

Figure 5. Molecular structure of the μ-CO_2 complex [MeSi{SiMe$_2$N(*p*-tol)}$_3$Zr{OSMe$_2$-κO)}(μ-O$_2$C)Ru(CO)Cp(CO)(SMe$_2$)] (**24a**) generated by the reaction of **6** with dimethyl sulfoxide. Interatomic distances and angles principally involving the tripodamide and carbonyl ligands and the cyclopentadienyl group are listed in Table 2 for comparison. Other selected parameters: Zr−O(1) 2.251(7), O(1)−S(1) 1.775(12), Zr−O(81) 2.222(6), Zr−O(82) 2.255(7), C(8)−O(81) 1.295(11), C(8)−O(82) 1.276(11), Ru−C(8) 2.083(9), Ru−S(2) 2.364(3) Å; O(1)−Zr−N(1) 171.7(3), N(2)−Zr−O(81) 152.6(3), N(3)−Zr−O(82) 152.5(3), O(81)−Zr−O(82) 58.3(2), O(1)−Zr−O(81) 82.8(2), Zr−O(1)−S(1) 131.5(4)°.

complex, [Cp$_2$Zr(Cl)(μ-O$_2$C)Ru(Cp*)(CO)] (Cp* = C$_5$Me$_5$), reported by Gibson et al.[48] The dimethyl sulfide molecule formed as a consequence of the sulfoxide deoxygenation is coordinated to the Ru atom, making this a chiral center. The metallacarboxylato unit in **24a** is almost symmetrically coordinated to the zirconium center [d{Zr−O(81)} 2.221(6) Å, d{Zr−O(82)} 2.255(7) Å] and together with the dmso ligand [d{Zr−O(1)} 2.251(7) Å] generates the hexacoordinate zirconium complex fragment, the coordination geometry of which may be viewed as being highly distorted octahedral.

The geometry of **24a** cannot be compared directly with that of its Zr−Ru precursor **6** (for which X-ray-quality crystals could not be obtained), but the corresponding parameters in the Zr−Fe heterobimetallic **5** may be assumed to be very similar to those of **6**, because, as shown in Table 3, all the parameters describing the coordination of the tripodal ligand in the two related titanium heterobimetallics, the Ti−Fe compound **3** and its Ti−Ru analogue **4**, are equal within experimental error. In an attempt to adapt to octahedral geometry, the mean N−Zr−N angle subtended by the tripodal ligand at zirconium was contracted from a value of 105.4(4)° in **3** to 102.0(3)° in **24a**. This was achieved by the lengthening of the mean Zr−N bond length from 2.078(9) Å in **5** to 2.133(7) Å in the insertion product **24a**, accompanied by a *decrease* in the corresponding N···N distance between the donor atoms from 3.305(12) Å in **5** to 3.286(10) Å in **24a**, and although this difference is of low significance, it contrasts with the significant *increase* in the corresponding mean N···N distance from 3.113(10) to 3.204(7) Å in going from **4** to to its isonitrile insertion product **17a**, in which the titanium atom adopts a tetrahedral coordination geometry (vide supra). In **24a**, it is again the flexibility at the bridgehead silicon atom that controls the "bite size" of the tripodal ligand, the decrease in N···N distance being produced

by a decrease in the mean Si−Si−Si angle from 105.6(1) to 104.3(2)° in going from **5** to **24a**.

The conformation of tolyl groups in **24a** is markedly asymmetric, with mean deviations from the idealized orthogonal disposition (vide supra) of −11.4° [ring C(11)], −32.1° [ring C(21)], and 13.3° [ring C(31)]; these rotations presumably minimize unfavorable contacts with the extra ligands at zirconium, and all contacts involving these rings are in the normal van der Waals range.

The complexes **23a−d** and **24a−c** have several very characteristic spectroscopic properties which aid the structural assignment. As a consequence of the generation of a chiral center at the late transition metal fragment, the ^{1}H and ^{13}C NMR resonances of the Si(CH$_3$)$_2$ groups in the tripod ligand are diastereotopically split. The coordination of the soft donor ligand RR′S at the Ru centers is the reason for the observation of the single ν(CO) infrared band at fairly low frequency (1924−1960 cm^{-1}). The chemical shifts of the ^{13}C NMR signals assigned to the μ-CO_2 units depend quite sensitively upon the presence or absence of the additional RR′SO donor at the Zr center. For **23a−d** they are observed at respectively δ 235.4, 232.0, 231.3, and 236.8 while the electronic readjustment within the molecule following the sulfoxide coordination at Zr leads to a significant shift of this signal to higher field [δ(^{13}C): **24a**, 225.1; **24b**, 225.6; **24c**, 225.0]. A study of this reaction employing compound **6** which was ^{13}C-labeled at the CO ligands provided support for the assumption of the role of these ligands as O acceptors and their transformation to the bridging CO_2 unit.

The oxygen transfer from the sulfur atom in the sulfoxides to a CO ligand was also proved by an ^{17}O NMR study of the reaction of **6** with 30% [17]O-labeled Ph(Me)SO [δ([17]O) = 0; standard dioxane[49−51]]. The chemical shift of the product signal of δ([17]O) = 344 for the labeled complex **23b** is indicative of an [17]O nucleus in a metallacarboxylato environment.[51]

Metal ion mediated oxygen transfer reactions involving sulfoxides have been known for some time,[52] the most thoroughly studied systems effecting this transformation being Pt(II) complexes in acidic solution[53−57] and low-valent group VI complexes which are transformed to the corresponding oxo species.[58−61] Deoxygenation of sulfoxides may also be achieved by some metal carbonyl derivatives under forcing conditions, generating CO_2 derived from metal-bound CO.[62−65] An important step in the labilization of the strong S−O bond is the addition of an electrophile to the oxygen atom. In reactions with early−late heterobimetallic complexes containing CO ligands coordinated to the late transition metal, *both* the electrophilic

(48) Gibson, D. H.; Mehta, J. M.; Sleadd, B. A.; Mashuta, M. S.; Richardson, J. F. *Organometallics* **1995**, *14*, 4886.

(49) Kalinowski, H.-O.; Berger, S.; Braun, S. *^{17}O und ^{29}Si-NMR-Spektroskopie*; Georg Thieme Verlag: Stuttgart, Germany, 1984.
(50) Gerothanassis, I. P.; Lauterwein, J. *Magn. Reson. Chem.* **1986**, *24*, 1034.
(51) Lycka, A.; Holecek, J. *J. Organomet. Chem.* **1985**, *65*, 2273.
(52) Kukushkin, V. Y. *Coord. Chem. Rev.* **1995**, *139*, 375.
(53) Bordwell, F. G.; Pitt, B. M. *J. Am. Chem. Soc.* **1955**, *77*, 572.
(54) Bird, C. W. *J. Chem. Soc.* **1968**, 1230.
(55) Kukushkin, V. Y.; Pankova, E. Y. *Koord. Khim.* **1989**, *15*, 531.
(56) Olah, G. A.; Malhotra, R.; Narang, S. C. *Synthesis* **1979**, 58.
(57) Kukushkin, V. Y.; Tkachuk, V. M.; Lebedev, V. B. *Zh. Neorg. Khim.* **1989**, *34*, 235 and references cited therein.
(58) Caradonna, J. P.; Reddy, P. R.; Holm, R. H. *J. Am. Chem. Soc.* **1988**, *110*, 2139 and references cited therein.
(59) Porohit, S.; Koley, A. P.; Prasad, L. S.; Manoharan, P. T.; Ghosh, S. *Inorg. Chem.* **1989**, *28*, 3735.
(60) Roberts, S. A.; Young, C. G.; Cleland, W. E.; Ortega, R. B.; Enemark, J. H. *Inorg. Chem.* **1988**, *27*, 3044.
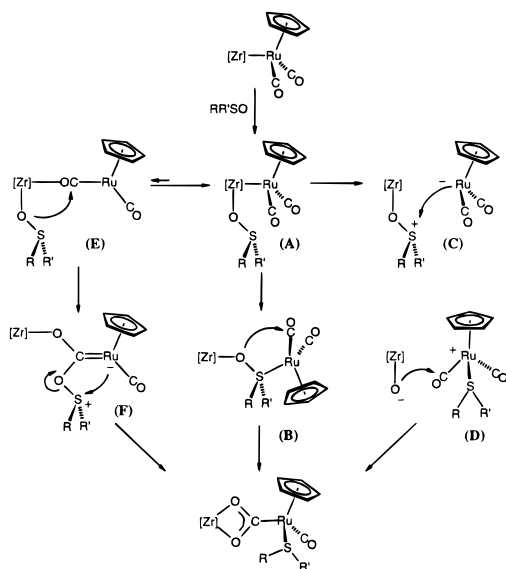(61) Nakamoto, M.; Tanaka, K.; Tanaka, T. *Inorg. Chim. Acta* **1987**, *132*, 193.
(62) Alper, H.; Keung, E. C. H. *Tetrahedron Lett.* **1970**, 53.
(63) Davies, S. G. *J. Organomet. Chem.* **1979**, *179*, C5.
(64) Alper, H.; Wall, G. *J. Chem. Soc., Chem. Commun.* **1976**, 263.
(65) Kukushkin, V. Y.; Moiseev, A. I. *Zh. Obshch. Khim.* **1990**, *60*, 692.

Scheme 5. Possible Mechanisms of the Oxygen Transfer from Sulfur to CO

activation of the substrate and the transfer to an oxygen acceptor ligand (CO) are possible within the coordination sphere of *one* molecule.

However, as is known from the large body of work involving the reactions of more reactive element oxides, such as amine oxides with metal carbonyls,[66–70] the CO carbon should have at least weakly electrophilic properties for such a reaction to occur. This is not the case in the metal carbonyl fragment present in **6**, which, due to the high polarity of the metal–metal bond, is to be viewed as being partially negatively charged. We therefore propose a mechanistic pathway for this transformation which involves an electrophilic activation not only of the sulfoxide by the Lewis acidic early transition metal but of the CO ligand as well (Scheme 5).

In an initial step, the substrate is thought to coordinate to Zr, thus polarizing and labilizing the Zr–Ru bond (**A**). Such a sulfoxide adduct may be isolated after adding dmso to the Ti–Ru complex **4** which does not effect the same oxygen transfer chemistry.[71] In reactions with inert element oxides, such as phosphine oxides, this may lead to the ionic dissociation of the metal–metal bond.[72] In the case at hand, there are two possible reaction pathways which mainly differ in the sequence of S–O

cleavage and C–O bond formation. One possible reaction pathway may proceed through insertion of the sulfoxide into the metal–metal bond in the same way as previously established for heteroallenes and isocyanides.[73] The coordination of the metal nucleophile and electrophile to the SO unit in **B** leads to its labilization and cleavage and the zirconium oxo fragment subsequently (or simultaneously) attacks a Ru-bound CO ligand to generate the carboxy bridge. Essentially the same reaction sequence may occur via the ion-pair intermediates **C** and **D**. Alternatively, we propose a rearrangement of the system (**A**) to generate an isomer containing an isocarbonyl link (**E**) which represents the species containing the activated CO. Such a structural unit has been observed previously by us and others in Zr–Mo heterodinuclear complexes containing the {CpMo-(CO)₃} fragment.[6,7,74–76] Intramolecular nucleophilic attack of the sulfoxide at the carbon atom induces the crucial C–O bond formation step to give an intermediate which rearranges—possibly via an oxycarbene species (**F**)—to the isolated reaction product. The O-transfer reaction proceeds extremely rapidly even at −70 °C which precluded a kinetic study or the detection of intermediates such as **B**–**F**.

Conclusions

The considerable thermal stability of the early–late heterodinuclear complexes **3**–**14**, which is a consequence of the coordination of the trisilylsilane-based tripodal amido ligand to the early transition metal, has allowed the study of both the structural characteristics and some aspects of the reactivity of the highly polar metal–metal bonds. Whereas the reactivity of these compounds toward isonitriles reflects their nature as "masked" electrophile–nucleophile pairs in reaction with unsaturated substrates, the deoxygenation of sulfoxides which has been established in the coordination sphere of the two metal centers provides an example of a more complex involvement of both metal fragments in the reaction with an organic substrate. The extraordinary mild conditions under which the oxygen transfer takes place are testimony to the cooperative nature of the bimetallic reactivity. Neither of the complex fragments alone effects these transformations.

(66) Alper, H. *Pure Appl. Chem.* **1980**, *52*, 607.
(67) Alper, H. *Pure Appl. Chem.* **1988**, *60*, 35.
(68) Shi, Y. L.; Gao, Y. C.; Shi, Q. Z.; Kershner, D. L.; Basolo, F. *Organometallics* **1987**, *6*, 1528.
(69) Gao, Y. C.; Shi, Q. Z.; Kershner, D. L.; Basolo, F. *Inorg. Chem.* **1988**, *27*, 191.
(70) Shen, J. K.; Gao, Shi, Q. Z.; Basolo, F. *Coord. Chem. Rev.* **1993**, *128*, 69.
(71) Schubart, M. Ph.D. Thesis, Universität Würzburg, 1997.
(72) Gade, L. H.; Fabre, S.; Memmler, H.; Kauper, U.; Schneider, A.; Bezougli, I.; Lutz, M.; Scowen, I. J.; McPartlin, M. *Chem.—Eur. J.*, in press.

(73) Memmler, H.; Kauper, U.; Gade, L. H.; Scowen, I. J.; McPartlin, M. *Chem. Commun.* **1996**, 1775.
(74) Longato, B.; Martin, B. D.; Norton, J. R.; Anderson, O. P. *Inorg. Chem.* **1985**, *24*, 1389.
(75) Sartain, W. J.; Selegue, J. P. *Organometallics* **1984**, *3*, 1922.
(76) Findeis, B.; Gade, L. H. Unpublished results.